Natural Resources Canada | Ressources naturelles Canada

GEOLOGICAL SURVEY OF CANADA
OPEN FILE 8752

Geoenvironmental characterization of ferroniobium slag, Saint Lawrence Columbium Mine, Oka, Québec

A.J. Desbarats, J.B. Percival, P. Pelchat, J. Sekerka, I. Bilot, I. Girard, and P. Gammon

2020

Canada

GEOLOGICAL SURVEY OF CANADA
OPEN FILE 8752

Geoenvironmental characterization of ferroniobium slag, Saint Lawrence Columbium Mine, Oka, Québec

A.J. Desbarats, J.B. Percival, P. Pelchat, J. Sekerka, I. Bilot, I. Girard, and P. Gammon

2020

© Her Majesty the Queen in Right of Canada, as represented by the Minister of Natural Resources, 2020

Information contained in this publication or product may be reproduced, in part or in whole, and by any means, for personal or public non-commercial purposes, without charge or further permission, unless otherwise specified.
You are asked to:
- exercise due diligence in ensuring the accuracy of the materials reproduced;
- indicate the complete title of the materials reproduced, and the name of the author organization; and
- indicate that the reproduction is a copy of an official work that is published by Natural Resources Canada (NRCan) and that the reproduction has not been produced in affiliation with, or with the endorsement of, NRCan.

Commercial reproduction and distribution is prohibited except with written permission from NRCan. For more information, contact NRCan at nrcan.copyrightdroitdauteur.rncan@canada.ca.

Permanent link: https://doi.org/10.4095/327565

This publication is available for free download through GEOSCAN (https://geoscan.nrcan.gc.ca/).

Recommended citation
Desbarats, A.J., Percival, J.B., Pelchat, P., Sekerka, J., Bilot, I., Girard, I., and Gammon, P., 2020. Geoenvironmental characterization of ferroniobium slag, Saint Lawrence Columbium Mine, Oka, Québec; Geological Survey of Canada, Open File 8752, 1 .zip file. https://doi.org/10.4095/327565

Publications in this series have not been edited; they are released as submitted by the author.

Cover photograph: Slag button from the SLC mine site. Photograph by A.J. Desbarats, June 2018. NRCan Photo Database number 2020-613.

FOREWORD

The emergence of new green technologies is driving increasing demand for advanced materials containing metals termed "critical" due to their scarcity or risk of supply disruption. However, potential environmental issues associated with the mining of many critical metals are not yet well understood. In order to address these knowledge gaps and Natural Resources Canada (NRCan) strategic priorities with respect to sustainable resource development, the Geological Survey of Canada (GSC) conducted a project on "Geoenvironmental Characteristics of Canadian Critical Metal Deposits" during the 2014-2019 cycle of the Environmental Geosciences Program. The objectives of the project were to characterize the chemistry of potentially hazardous trace elements in mine wastes and waters, and to understand their mobilization, transport, and fate in the environment. The project focused on carbonatite intrusions, an important class of mineral deposit hosting critical metals including niobium (Nb) and rare earth elements (REE). Because carbonatite deposits exhibit many common geological and mineralogical features, their mine wastes will share similar environmental characteristics as well. Studying these wastes at historical mine sites provides useful benchmark information that can improve environmental assessment predictions for new mines hosted in carbonatite deposits elsewhere. The past-producing Saint Lawrence Columbium mine near Oka, Québec, is an example of carbonatite-hosted critical metal deposit that serves here as an analogue for other carbonatite deposits currently under consideration for development in Canada and abroad. This report is specifically concerned with the environmental signature of ferroniobium slag, a mine waste produced by the aluminothermic conversion of pyrochlore concentrate to ferroniobium alloy. It describes the physical characteristics of the slag, its mineralogy, bulk chemistry, and radioactivity, as well as the chemistry of its leachate. The results of this investigation promote the sustainable development of critical metal resources by making new open data and knowledge available to stakeholders. This information will help to better predict and mitigate environmental risks associated with resource development, and thereby to improve the efficiency of the regulatory approval process for future mining projects hosted in carbonatites.

SUMMARY

Between 1961 and 1976, the St. Lawrence Columbium mine produced pyrochlore concentrate from a niobium-bearing carbonatite deposit near Oka, Québec. Beginning in 1971, the pyrochlore concentrate was converted into ferroniobium alloy through an aluminothermic reduction process, which also yielded slag as a waste product. Uranium and thorium occurring as impurities within the pyrochlore were preferentially sequestered in the slag. As a result, the slag represents Technologically Enhanced Naturally Occurring Radioactive Material (TENORM) requiring a long-term management solution.

Slag at the mine was deposited on the surface and has been exposed to the elements for approximately 45 years. Much of the slag exhibits an advanced degree of weathering. The slag consists of an assemblage of high-temperature mineral phases including hibonite, grossite, and perovskite, as well as amorphous glass. The minerals deviate significantly from their ideal compositions as they incorporate rare earth and other trace elements including uranium and thorium. Geochemically, the slag is composed mainly of aluminum, calcium, and sodium from reagents, and impurities from the pyrochlore concentrate including titanium, silicon, zirconium, uranium, thorium, and rare earth elements, as well as unrecovered niobium.

A ground-based spectral radiometric survey was conducted on a longitudinal transect through the slag disposal area. Equivalent uranium concentrations ranged between 455 and 1616 ppm, with a median value of 1069 ppm. Equivalent thorium concentrations ranged between 607 and 5059 ppm, with a median value of 2101 ppm. Assuming secular equilibrium within the decay series, total activity concentrations of the slag varied between 126 and 417 Bq/g, with a median of 304 Bq/g. These results are consistent with detailed radiological analyses for U-238, U-235, Th-232 and their daughter products performed on three selected slag samples.

An on-site field-scale leach test was conducted on three 220 L barrels of coarse vesicular slag open to natural precipitation. The experiment ran from June of 2017 to November of 2018 during which time collected leachate was sampled six times. The leachate had a near constant pH of 9.2 while specific conductance values varied between 1191 and 3280 µS/cm. Leachate chemistry did not stabilize during the test, likely because seasonal freeze-thaw cracking of the slag was regularly exposing fresh surfaces to chemical weathering. The main solutes were sodium and bicarbonate. Fluoride concentrations varied between 16.8 and 45.6 mg/L. Dissolved aluminum and uranium concentrations reached as high as 8173 and 65 µg/L, respectively. Although uranium is hosted by most minerals in the slag, it is released mainly by the weathering of unstable glass phases.

This investigation of slag geochemistry at the former St. Lawrence Columbium mine, provides new geoscience data and knowledge useful for the environmental assessment of future carbonatite-hosted niobium mining projects. The information will allow proponents and other stakeholders to anticipate potential environmental impacts associated with new resource development and to plan appropriate mitigation measures accordingly.

TABLE OF CONTENTS

FOREWORD v

SUMMARY vii

1. INTRODUCTION 1
   1.1 Background 1
   1.2 Saint Lawrence Columbium Mine 1
   1.3 Potential Environmental Risks from Mine Wastes 3
   1.4 Previous and Related Studies 6
   1.5 Objectives and Scope 6
   1.6 Accompanying Data Files 7
   1.7 Acknowledgments 7

2. STUDY AREA 8
   2.1 Climatic and Physiographic Setting 8
   2.2 Geological Setting 10
   2.3 Economic Geology 12
   2.4 Ferroniobium Conversion 13

3. METHODOLOGY 14
   3.1 Site Description 14
   3.2 Radiometric Survey 16
   3.3 Field-Scale Slag Leach Test Cells and Leachate Sampling 16
   3.4 Laboratory Methods 20

4. RESULTS 22
   4.1 Physical Description of the Slag 22
   4.2 Mineralogy 23
   4.3 Geochemistry and Radiochemistry 25
   4.4 Radiometric Survey of the Slag Disposal Area 29
   4.5 Slag Leachate Chemistry 31

5. DISCUSSION 41
   5.1 Interpretation of Leach Experiment Results 41
   5.2 Comparisons with Results of Previous Studies 49

6. SUMMARY AND CONCLUSIONS 54

REFERENCES 55

APPENDIX 60

1. INTRODUCTION

1.1 Background

With the emergence of new green technologies, there is increasing demand for advanced materials containing metals termed "critical" due to their scarcity or risk of supply disruption. Niobium (Nb) and rare earth elements (REEs) are critical metals often mined in carbonatite deposits (Richardson and Birkett, 1996; Berger et al., 2009; Simandl and Paradis, 2018). Carbonatites are defined as igneous rocks composed of at least 50% carbonate minerals such as calcite, dolomite, and ankerite. They typically form the central core of alkaline intrusive complexes (Simandl and Paradis, 2018). The main Nb ore mineral is pyrochlore whereas bastnaesite and monazite are the main REE economic host minerals (Verplanck et al, 2014; Mitchell, 2015). The magmatic differentiation processes that concentrate Nb and REE in these minerals also concentrate other incompatible elements, such as uranium (U) and thorium (Th), in the same hosts (Verplanck and Van Gosen, 2011). Thus, anomalous values of U and Th are common in carbonatites and represent an environmental concern (Weng et al., 2013; Huang et al., 2016). However, there have been few published investigations of environmental issues associated with the development of carbonatite deposits (Edahbi et al., 2018a, 2018b). Because a number of carbonatites in Canada are being considered as sources of Nb or REEs (or both), greater understanding of potential environmental effects is needed in order to better inform the regulatory approval process for these and similar projects. Such knowledge could reduce uncertainty associated with their environmental impact assessments.

Carbonatite-hosted Nb and REE deposits (Simandl and Paradis, 2018) form a class of mineral deposits defined by shared geological, mineralogical, and geochemical characteristics. Wastes produced by the mining of different carbonatite deposits, therefore, are likely to share similar environmental characteristics. Studying these wastes at historical mine sites provides transferable benchmark information that can be used to improve predictions and mitigation measures for environmental assessments of new mines in carbonatite deposits elsewhere. The former Saint Lawrence Columbium (SLC) mine near Oka, Québec, is an example of carbonatite-hosted critical metal deposit and it was studied here as an analogue for other carbonatite deposits currently under consideration for development in Canada and abroad.

1.2 The Saint Lawrence Columbium Mine

Spurred by the 1950s uranium boom, the discovery of radioactive minerals near Oka prompted the St. Lawrence River Mining syndicate to stake a large portion of the surrounding area in early 1954. While the original exploration target was uranium, the greater economic significance of the niobium (columbium) content of the Oka carbonatite soon became apparent after drilling revealed the presence of several mineralized lenses and large bodies of low-grade pyrochlore-bearing rocks (Carbonneau and Caron, 1965). However, the challenge was to develop a viable pyrochlore concentration process. Research carried out at the École Polytechnique in Montréal and the Department of Mines and Technical Surveys in Ottawa eventually led to the design and construction of a pilot plant in 1959. The plant was able to achieve a 50 % Nb_2O_5 concentrate

Figure 1: View of the mine site in 1967, looking south toward the Lac des Deux Montagnes. The photograph shows the newly completed headframe and the tailings disposal area in the foreground. Photograph from SLC (1967).

from a head grade of 0.4 % Nb_2O_5. After the original mining group merged with another company, the newly formed St. Lawrence Columbium and Metals Corporation (SLC) started construction of a 500 tons/day mill on the site and negotiated a two-year contract for 1 million pounds of Nb_2O_5 concentrate (Vallières, 1989). Mining and concentrate production started in October of 1961. At that time, SLC's Oka mine was the world's first primary producer of Nb_2O_5 as well as the single largest producer (Carbonneau and Caron, 1965).

Initially, ore was obtained from two open pits. Underground mining started in 1965 with access to the workings from an adit in the wall of the deeper pit. Following the completion of a 410 m (1345 ft.) shaft in late 1966, production shifted completely underground in 1968 (Figure 1). In 1971, the shaft was deepened to 586 m (1922 ft.) in order to access higher-grade reserves at depth. Throughout the mine life, mill capacity was gradually increased to 1700 tons/d in 1967, 2200 tons/d in 1972, and then 3000 tons/d in 1975. At the same time, modifications to the milling process improved pyrochlore recovery (Carbonneau and Caron, 1965; SLC, 1967). With research funding from the federal government, a new lower cost and higher efficiency concentrator flow-sheet was developed and plans were made to reprocess mine tailings containing an estimated 12 million pounds of Nb_2O_5 (SLC, 1971). Starting in 1972, the original milling process was phased out in favour of the new process, which was implemented in a parallel milling circuit (SLC, 1972). Meanwhile, in 1969, the company constructed a small-scale plant for custom production of ferroniobium alloy, the form of niobium consumed by most end users (SLC, 1969). In order to meet increasing demand from the steel industry, the company began building a new full-scale ferroniobium conversion facility in 1971 (SLC, 1971). Thereafter, the company marketed both

pyrochlore concentrate and ferroniobium. The company also explored opportunities to market useful milling by-products including high-purity calcite, magnetite, and apatite as a source of phosphate fertilizer and rare earth elements (SLC, 1971).

In latter years, despite all the measures aimed at increasing the profitability of its operation, the company was struggling financially because of competition from new lower-cost and higher-grade producers in Brazil. In 1976, after a labour dispute closed the mine, SLC went into liquidation (Vallières, 1989).

During its 15-year life, SLC's Oka mine produced a total of 6.35 million tons of ore at an average grade of 0.46 % Nb_2O_5 (NIOCAN, 2010). Annual production data are summarized in Table 1. At the time of closure, reserves (noncompliant with NI 41-103) were estimated at 21.7 million tonnes of ore grading 0.44 % Nb_2O_5 (NIOCAN, 2010). Currently (in 2020), the mine site (Figure 2) is owned by the municipality of Oka while the mining rights belong to Niocan Inc. (http://www.niocan.com).

1.3 Potential Environmental Risks from Mine Wastes

During environmental hearings for Niocan's proposed development of an extension of the SLC niobium deposit, public concerns were centered on radioactive mine wastes and their impact on groundwater quality (BAPE, 2002; 2005). Groundwater is the sole source of potable supply for local inhabitants and is tapped extensively for irrigation of market gardens and orchards in the surrounding area.

Trace metals of potential concern associated with carbonatite-hosted Nb-REE deposits include U, Th, and their radioactive decay products (Paschoa, 1998), as well as Nb and REE (USEPA, 2012; Verplanck et al., 2014; Schultz et al., 2017). Although these metals usually are hosted by relatively stable and insoluble minerals, mining activities can significantly enhance risks to groundwater quality because, in waste rock piles and fine-grained tailings, the surface area of reaction between contact waters and contaminant-bearing minerals is greatly increased. A radiation hazard also may be created because the ore beneficiation process by which pyrochlore concentrate is produced also concentrates naturally occurring U and Th (Paschoa, 1998). The subsequent ferroniobium conversion of the concentrate redistributes U and Th from stable pyrochlore to less stable phases in waste slags (Mitchell and Mariano, 2016). To date, however, there has been limited published information on the geoenvironmental signature of ferroniobium slag or its leachate, important waste streams associated with carbonatite-hosted niobium deposits.

Table 1: Annual production statistics for the St. Lawrence Columbium and Metals Corporation mine at Oka, Québec. Beginning in 1971, the company marketed its niobium production as Nb_2O_5 concentrate or as ferroniobium (FeNb).

Year	Ore Milled (tons)	Nb_2O_5 Produced in concentrate (lbs)	Ore Grade % Nb_2O_5	Reference
1961	n.a.*	134 006	n.a.	C&C, 1965[3]
1962	172 767	775 313	0.43	SLC, 1962
1963	291 403	1 393 536	0.40	SLC, 1963
1964	321 585	2 091 725	n.a.	SLC, 1964
1965	383 553	2 203 985	0.43	SLC, 1966
1966	406 698	2 647 667	0.47	SLC, 1966
1967	369 642	2 368 225	n.a.	SLC, 1967
1968	360 194	2 005 989	n.a.	SLC, 1968
1969	475 201	3 059 052	n.a.	SLC, 1969
1970	724 345	4 886 957	n.a.	SLC, 1970
1971	408 500	n.a.	n.a.	SLC, 1971
1972	589 147	n.a.	n.a.	SLC, 1972
1973	461 741[1]	n.a	n.a.	
1974	461 741	n.a.	n.a.	
1975	461 741	n.a.	n.a.	
1976	461 742	n.a.	n.a.	
Total	6 350 000	39 725 600[2]	0.46	NIOCAN, 2010

*n.a. Data not available

[1] Estimates for 1973-1976

[2] Estimate of equivalent Nb_2O_5 in concentrate assuming a mill recovery of 68%

[3] Carbonneau and Caron (1965), Table VI

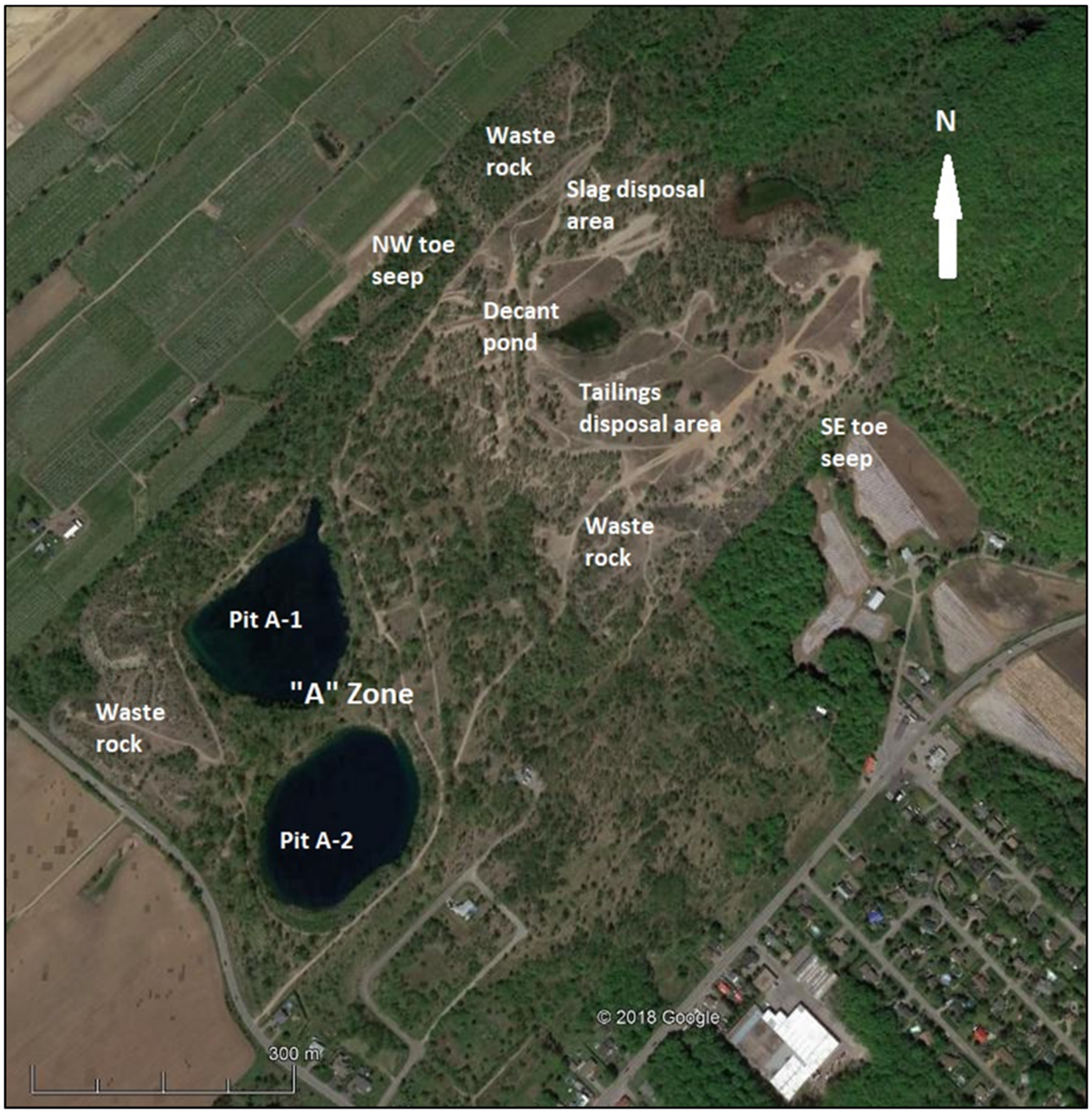

Figure 2: Satellite image with annotations indicating the main features of the former SLC mine site in 2018. Google Earth Image used with permission.

1.4 Previous and Related Studies

In response to public concerns related to the abandoned SLC site and to possible geogenic (natural) contamination associated with the broader Oka carbonatite complex, the GSC conducted an airborne radiometric survey of the area (GSC, 1996; Ford et al., 2001) while local health authorities performed surveys of residential radon (RRSSSL, 1998) and uranium in domestic wells (RRSSSL, 1999). Limited investigations of the SLC site were carried out in support of the environmental impact assessment for the proposed Niocan niobium mine located approximately 1.5 km to the west (BAPE, 2002, 2003, 2005; and supporting documents). As part of the GSC project on the geoenvironmental characteristics of the Oka carbonatite-hosted Nb-REE deposit, a companion open file report has been prepared on the geochemistry of mine tailings and their seepage (Desbarats et al, 2020). Reports on the mineralogy of the different types of mine waste (J. B. Percival, personal communication) and on pit lake water chemistry (M. B. Parsons, personal communication) are in preparation. Master's theses on Oka slag mineralogy and leaching (Balkwill-Tweedie, 2020) and on mine waste mineralogy and leaching (Des Roches, 2020) have been completed recently. In the summer of 2017, the Ministère de l'Énergie et des Ressources Naturelles du Québec (MERNQ) carried out site characterization studies as the first phase of its remediation plans for the former SLC mine (WSP, 2018).

1.5 Objectives and Scope

An aluminothermic conversion process is used to produce ferroniobium (FeNb) alloy from pyrochlore concentrate. The slag residual is generally radioactive as it scavenges U and Th impurities originally hosted within the pyrochlore. Since there is little published information on the environmental signature of FeNb slag, this study seeks to address knowledge gaps through an investigation of the slag deposited at the former SLC mine site. Its objectives are to address the following questions:

1. What are the mineralogical, geochemical, and radiological characteristics of FeNb slag?

2. What are the geochemical characteristics of leachate from the slag?

3. What are the potential contaminants of concern in slag leachate?

4. What are the geochemical processes that may control the chemistry of slag leachate?

The scope of the study includes grab sampling of representative slag material, a spectral radiometric survey of the slag disposal area, and a field-scale slag leach test experiment. Samples of slag leachate were analyzed for a full suite of inorganic chemical parameters, including uranium and thorium. However, they were not analyzed for radioactive decay products of ^{238}U and ^{232}Th, including radon, nor were they analyzed for microbiological parameters.

1.6 Accompanying Data Files

This report is accompanied by four data files in Microsoft Excel® format. The files are described as follows:

- of_8752_slag chemistry.xlsx: file containing chemical analyses for three slag samples and one sample of pyrochlore concentrate.
- of_8752_slag radiochemistry.xlsx: file containing radiometric analyses for three slag samples and one pyrochlore concentrate sample.
- of_8752_radiometric profile.xlsx: file containing radiometric survey results.
- of_8752_leachate chemistry.xlsx: file containing analytical results for slag leachate chemistry.

1.7 Acknowledgments

This project was funded by the Environmental Geosciences Program of the Geological Survey of Canada. Leachate chemistry analyses were performed by Pierre Pelchat, Isabelle Girard, and John Sekerka under the supervision of Paul Gammon. Mineralogical work was carried out by Katherine Venance, Igor Bilot, and Thomas McLoughlin-Coleman under the supervision of Jeanne Percival. Additional technical support was provided by Jacques Pinard and Eric Potter. The authors would like to thank Robert Garrett for his helpful comments on a draft version of this report.

2. STUDY AREA

2.1 Climatic and Physiographic Setting

The former St. Lawrence Columbium mine (lat. 45.502°; long. 74.029° W) is located near Oka, Québec, approximately 36 km west of downtown Montréal. The village of Oka is part of the Deux Montagnes Municipalité Régionale de Comté (MRC), in the Basses Laurentides administrative region of Québec. The mine site is readily accessed from Montréal via highways 640 and 344.

The study area falls within the "Humid Mid-Cool Temperate" (MCTh) ecoclimatic region, which is characterized by warm summers and relatively mild winters (Strong et al., 1989). Between April and November, mean daily temperatures are above 0°C. At Environment Canada's Oka weather station, 3.2 km from the mine site, the mean annual temperature is approximately 6.0°C. The mean summer (July) temperature is 20.3°C and the mean winter (January) temperature is -10.9°C. Monthly precipitation, usually in excess of 70 mm, is fairly evenly distributed throughout the year. Mean annual precipitation is approximately 1107 mm including 871 mm of rainfall and 236 mm of snowfall equivalent. Climate Normals for the Oka weather station are presented in Table 2.

The mine site lies within the Saint Lawrence Lowlands ecoregion, which includes the valleys of the Ottawa and Saint Lawrence rivers. The ecoregion extends from the Frontenac Axis, near Brockville in the west, to Québec City in the east. It is bounded by the Laurentian Highlands to the northwest and by the Eastern Québec uplands to the southeast (Ecozones, 2014).

Most of the lowlands are underlain by flat-lying Paleozoic strata resting on Precambrian bedrock. In the study area, however, Precambrian inliers form the Oka, Saint-André, and Rigaud Hills. Elevations range from 230 m on the highest of the Oka hills to 22 m on nearby Lac des Deux Montagnes. Beyond the study area, the Monteregian Hills form an elongated east-west trend of isolated features rising sharply above the surrounding plain and reaching elevations sometimes exceeding 400 m. They represent resistant erosional cores of early Cretaceous alkaline igneous intrusions related to the Oka and Saint-André carbonatites.

The landscape of the Saint Lawrence lowlands has been shaped by the last continental glaciation, followed by the Champlain Sea incursion and retreat, and subsequent river erosion and deposition. Most of the lowlands are blanketed by glacio-marine clay of the Champlain Sea, which can reach a thickness of over 60 m. More elevated areas, such as the Oka Hills, are covered by glacial till resting on bedrock. Reworking of the till by wave action during the marine retreat has left numerous sandy terraces representing former strand lines. Gleysols are developed on the level, poorly drained, Champlain Sea deposits whereas humo-ferric podzols and dystric brunisols are found on morainal uplands and beach terraces (Ecozones, 2014).

The broader study area is drained by the Rivière du Nord, the Rivière Rouge and the Rivière du Chêne. On the west, the mine area is drained by a ditch, which eventually joins the Ruisseau Rousse. On the east, the site is drained by a small creek known as the "effluent Saint-Pierre" (WSP, 2018). Both these water courses flow to the Grande Baie on the Lac des Deux Montagnes. Groundwater flow patterns in the study area (Nastev et al., 2005) are controlled by bedrock

topography and permeability. Most recharge occurs in the Oka and Saint-André hills from which groundwater flows radially outward before discharging in local streams or in the Lac des Deux Montagnes.

Table 2: Climate Normals (1981-2010) for the weather station at Oka, Québec (lat. 45° 30.00', long. 74° 04.00' W, elevation 91.4 m a.s.l.). Data from ECCC (2018).

Month	Daily Average (°C)	Daily Maximum (°C)	Daily Minimum (°C)	Rainfall (mm)	Snowfall (cm)	Precipitation (mm)
Jan	-10.9	-6.1	-15.7	30.2	59.9	90.2
Feb	-8.9	-3.6	-14.1	21.4	50.9	72.3
Mar	-2.9	2.1	-7.9	33.9	37.7	71.6
Apr	5.7	11.0	0.4	78.1	10.9	88.7
May	12.7	18.7	6.7	93.3	0	93.3
Jun	17.8	23.6	12.0	105.4	0	105.4
Jul	20.3	26.0	14.6	97.5	0	97.5
Aug	19.0	24.9	13.2	99.9	0	99.9
Sep	14.5	20.3	8.8	95.3	0	95.3
Oct	7.7	12.6	2.8	102.6	2.5	105.1
Nov	1.3	5.1	-2.5	78.0	20.0	97.9
Dec	-6.4	-2.2	-10.4	35.3	54.3	89.6
Year	**5.8**	**11.0**	**0.6**	**871**	**236**	**1107**

The dominant vegetation in the ecoregion is mixed-wood forest consisting of sugar maple, yellow birch, eastern hemlock, and eastern white pine, with beech appearing on warmer sites. Dry sites are dominated by red and eastern white pine, and red oak. Wetter sites support red maple, black ash, white spruce, tamarack, and eastern white cedar. Characteristic wildlife includes white-tailed deer, black bear, raccoon, skunk, squirrel, and chipmunk (Ecozones, 2014).

In the study area, agriculture is the most important land use with numerous apple orchards, market gardens, and vineyards. Maple sugar bushes are found on the wooded hills. Because of its proximity to the Greater Montréal Area, farmland around Oka is threatened by urban expansion.

2.2 Geological setting

The Oka carbonatite complex has been studied extensively because of its rare and unusual rock types and minerals. Gold et al. (1967) and Gold and Vallée (1969) provide an overview of the geology of the complex and of the St. Lawrence Columbium mine, which is summarized here.

The Cretaceous (113-127 Ma, Chen and Simonetti, 2013) Oka carbonatite complex belongs to the suite of alkaline intrusions that form the Monteregian Hills. It was emplaced within a Precambrian inlier of Grenville gneisses and anorthosites metasomatically altered (fenitized) locally in contact with the intrusion. The inlier is surrounded by gently dipping basal Paleozoic strata represented by Potsdam conglomerates, and sandstones of the Cambrian Covey Hill and Cairnside Formations. The carbonatite complex is clearly revealed by airborne radiometric surveys as an area of high equivalent thorium concentrations (Figure 3).

The Oka complex consists of two ring-shaped structures forming a distorted "figure 8" 7.2 km long by 2.4 km wide and aligned in a NW-SE direction (Figure 4). The carbonatites are intercalated with ring-dykes and cone-sheets of silica-undersaturated and ultramafic rocks. In the larger northern ring, dips of the units are outward on the margins of the complex and inward toward the centre. In the smaller southern ring, dips of the units are outward but steepen toward the margins. The main geological units within the complex belong to four distinct series:

- Carbonatites. Most of the carbonatite, including the core of the complex, consists of a coarse-grained calcite-carbonatite (sövite) although dolomite-carbonatite (rauhaugite) is found in the northwest of the complex. The sövites typically contain 70-90 % calcite and variable amounts of accessory biotite, sodian augite, richterite, apatite, nepheline, monticellite, melilite, magnetite, perovskite, pyrochlore, niocalite, pyrite, and pyrrhotite.
- Melteigite-Ijolite-Urtite series. Rocks of this series are composed of nepheline and variable amounts of mafic minerals such as alkali pyroxene and amphiboles, biotite, and melilite. Urtite contains over 70% nepheline whereas melteigite, the mafic end-member, consists mostly of pyroxenes. Most rocks are ijolites containing up to 50 % nepheline.
- Okaite-Jacupirangite series. These ultramafic rocks are composed essentially of melilite, hauyne, and pyroxene with accessory biotite, perovskite, apatite, magnetite, and calcite. Within the complex, the series exhibits considerable compositional variation.
- Alnoites. Alnoite and breccias with an alnoite matrix form late-stage dykes and plugs around the complex and in the surrounding gneisses. Alnoites are porphyritic ultramafic rocks containing phenocrysts of biotite or phlogopite, augite, olivine, and magnetite in a matrix of melilite, phlogopite, perovskite, calcite, and apatite. Here, the melilite has been replaced by calcite and perovskite is largely absent.

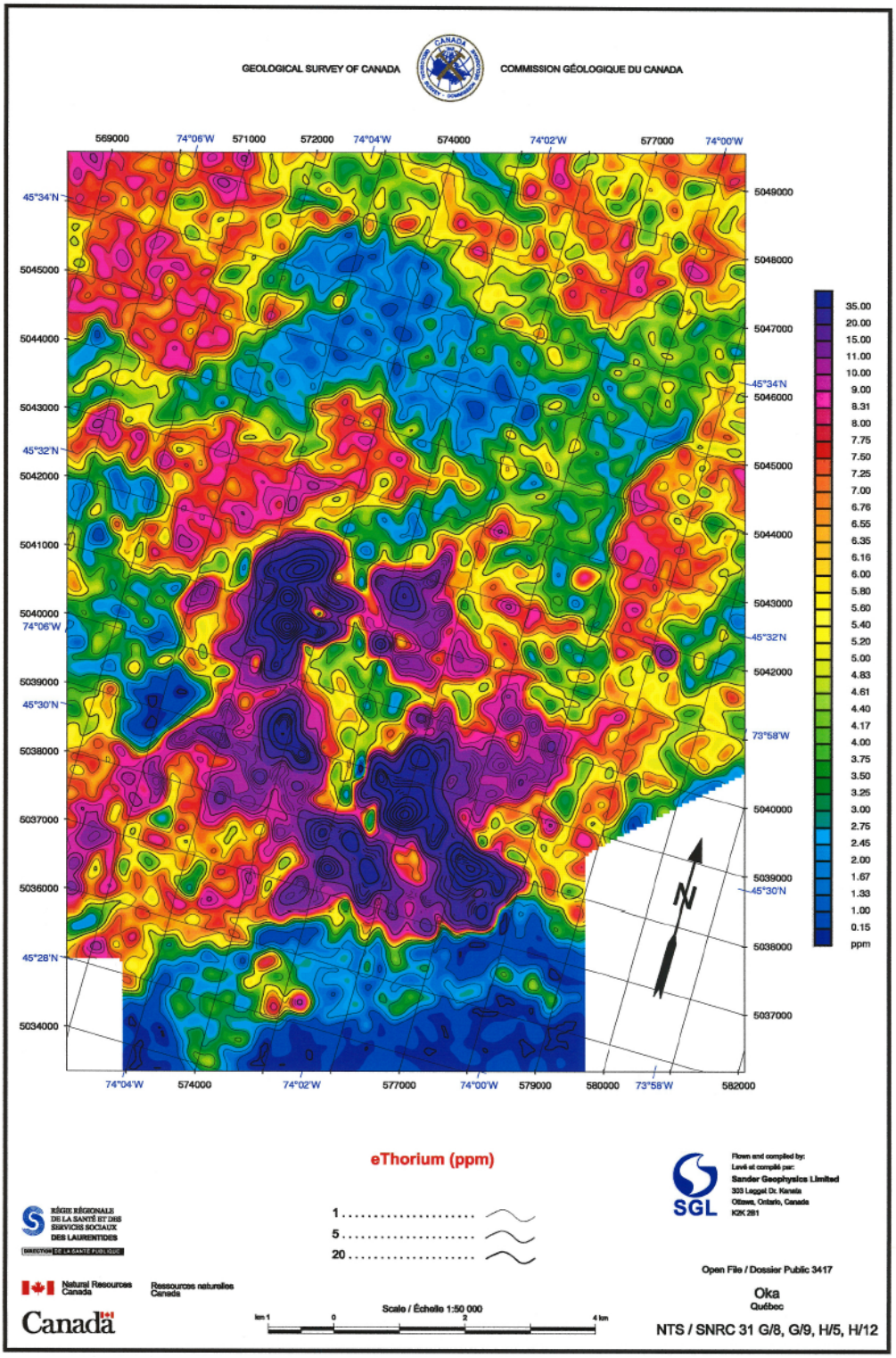

Figure 3: Airborne radiometric map of equivalent thorium concentrations in the study area. The Oka Carbonatite Complex is clearly revealed by areas of high concentrations shown in deep purple. Equivalent uranium concentrations exhibit a similar anomalous pattern (GSC, 1996).

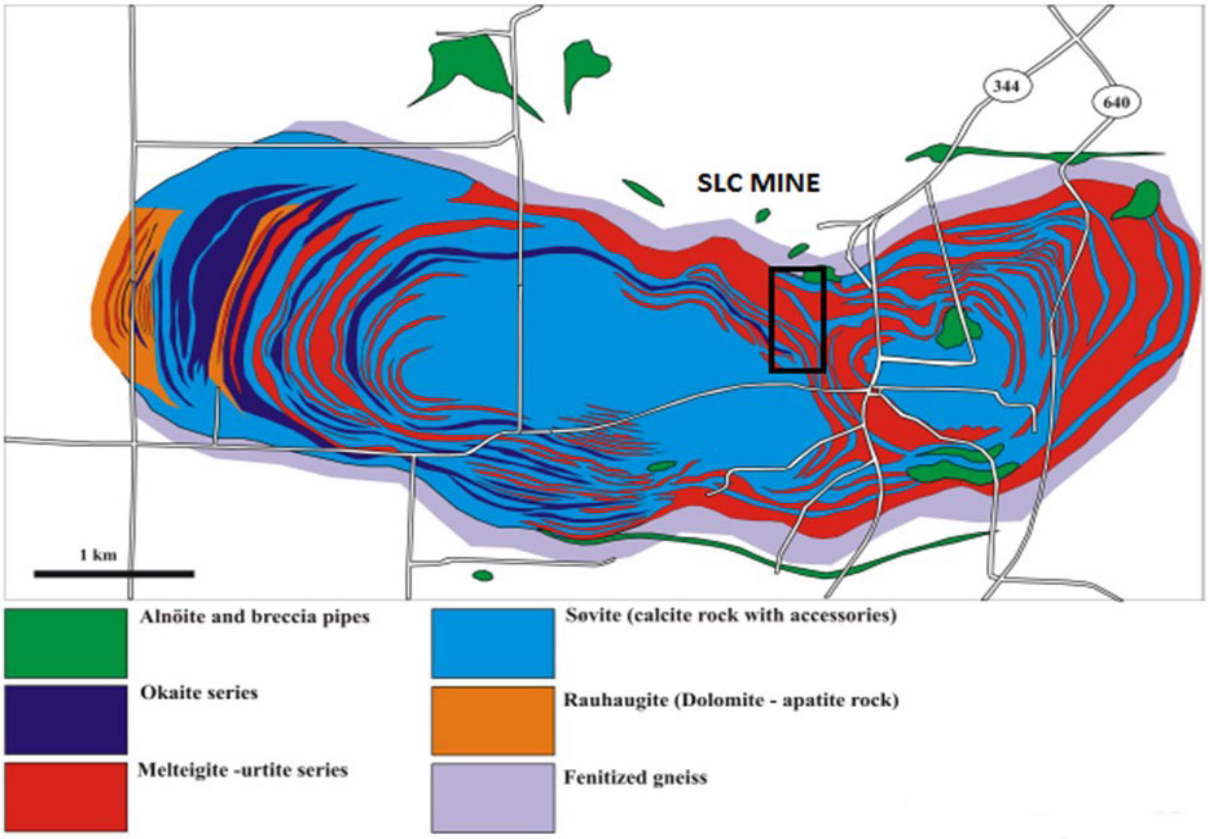

Figure 4: Simplified geology of the Oka Complex (modified from Figure 11 of Lentz et al., 2006). The black rectangle indicates the location of the SLC site.

2.3 Economic geology

All the rock types within the Oka complex contain some degree of primary Nb mineralization of magmatic origin. However, the main economic host rock of Nb is sövite and pyrochlore in the main Nb mineral. For the purposes of grade control during mining, sövites have been classified into four main types (Gold et al., 1967):

1. Early stage Nb-poor sövite containing monticellite (0.03-0.10 % Nb_2O_5)
2. Middle stage Nb-rich sövite (0.20-0.80 % Nb_2O_5)
3. Other sövite (0.10-0.50 % Nb_2O_5 and up to 1.50 % Nb_2O_5 when biotitized)
4. Late stage Nb-poor and REE-enriched sövite (0.02-0.05 % Nb_2O_5)

The silicate rocks generally contain less than 0.15 % Nb_2O_5 although grades in biotitized ijolite may reach 2 % Nb_2O_5 (Gold et al., 1967).

The SLC mine was developed on the "A" zone (Figure 2), which consists of sövites intruded by tabular bodies and irregular masses of ijolites and some okaite (Gold et al., 1967). The main constituents of the sövite are calcite (70-85 %) and apatite (5-15 %), with variable amounts of biotite (3-15 %), pyroxene (0-10 %), monticellite (0-10 %), magnetite (0.5-5 %), sulfides (1-3 %) mainly as pyrite, pyrrhotite or sphalerite, and pyrochlore (0-1 %). Because all sövite types contain some pyrochlore, ore-waste limits were essentially economic and mining required stringent grade control measures based on sövite type (Carbonneau and Caron, 1965; Gold et al., 1967).

Pyrochlore is the main Nb-bearing mineral at the SLC mine. Other Nb-bearing minerals uniquely found within the Oka complex are perovskite (latrappite) and niocalite (Gold et al., 1967). However, neither mineral is of economic significance. Pyrochlore is a niobium oxide having the general formula (Zurevinski and Mitchell, 2004): $A_{16-x}B_{16}O_{48}(O,OH,F)_{8-y} \bullet z\,H_2O$ where x and y are vacant sites in the unit cell, and x, y, and z are non rational numbers. The pyrochlore structure can accommodate a wide variety of cations in the *A* and *B* sites. At the SLC mine, *A* site cations include Ca, Na, REE, U, Th, Sr, Mn, and Y whereas the *B* sites are occupied mainly by Nb, with Ti, Ta, Zr, and Fe (Gold et al., 1967). Because of these substitutions, pyrochlore compositions are extremely variable at the SLC mine and elsewhere within the Oka complex (Carbonneau and Caron, 1965; Gold et al., 1967; Petruk and Owens, 1975; Zurevinski and Mitchell, 2004). Primary pyrochlore at the SLC mine occurs mainly in disseminated form in layers or pods of specific rock types, particularly biotite-pyroxene sövite and monticellite sövite (Gold et al., 1967). Pyrochlores in these unaltered sövites contain from 47 to 66 % Nb_2O_5. Primary pyrochlore may also contain up to 0.72 % U_3O_8 and 1.51 % ThO_2 (Carbonneau and Caron, 1965). Deuteric pyrochlore is found in hydrothermally altered and biotitized zones. Although Nb grades may be higher in these zones they were avoided because the ore responded poorly to the milling process. Deuteric pyrochlore may contain up to 1.83 % U_3O_8 and 7.23 % ThO_2 (Gold et al., 1967). Uranian pyrochlore and uranpyrochlore from the SLC mine may contain up to 15.11 % and 24.79 % U_3O_8, respectively (Petruk and Owens, 1975). Mill concentrate contained on average 0.10 % U_3O_8 and 0.23 % ThO_2 (Gold et al., 1967, Table IV).

2.4 Ferroniobium conversion

A detailed description of the ferroniobium (FeNb) conversion process can be found in Gupta and Suri (1994). A brief generic description of the process is given by the online Encyclopedia Britannica (https://www.britannica.com/technology/niobium-processing): *"Pyrochlore concentrates are commonly reduced to ferroniobium through an aluminothermic process. In this process, the concentrate is mixed with hematite (an iron ore), aluminum powder, and small quantities of fluorspar and lime fluxes in a rotary mixer and then unloaded into steel containers lined with magnesite refractory bricks. Here the charge is placed in circular concave pits made of a mixture of lime, fluorspar, and silica sand, and reduction is initiated by the ignition of a mixture of aluminum powder and sodium chlorate or barium peroxide. The exothermic reaction lasts about 15 to 30 minutes, and the temperature reaches about 2,400°C (4,350°F). Most of the gangue impurities from the concentrate, including all the thorium and uranium oxides, enter the molten slag. When the reaction is finished, the slag is tapped off and the vessel is lifted, leaving the metal to solidify in the sand. The ferroniobium alloy is then crushed to particle sizes of 10 millimetres (about three-eighths of an inch) for marketing. The content of this alloy is 62–69 percent niobium, 29–30 percent iron, 2 percent silicon, and 1–3 percent aluminum."*

Figure 5: Ferroniobium production at the Niobec mine near St-Honoré, QC. Photograph from http://niobec.com/2014/11/20-ans-transformation-niobec/.

Based on information provided in the environmental assessment report for the proposed nearby Niocan mine project (BAPE, 2002, Figure 5, p.36), the conversion process yields 0.54 tonnes of FeNb and 1.38 tonnes of slag for each tonne of pyrochlore concentrate. Figure 5 shows a solidified slag "button" being removed from a concave foundry pit.

3. METHODOLOGY

3.1 Site description

Slag waste covers an area of approximately 6600 m^2 (WSP, 2018) in the northwest corner of the SLC property (Figure 2). Buttons of slag (Figure 6) broken into large chunks have been bulldozed into heaps on the levelled top of a waste rock pile (Figure 7). The total amount of slag is estimated at 4000 to 6000 tonnes (BAPE, 2002). In addition to the slag, numerous rusting steel drums containing what appears to be foundry sand and a glassy material are scattered about the area.

Figure 6: A rare comparatively intact button of slag found on the SLC site. Diameter of the button is about 1.5 m (5 ft.). The card is 8 cm across. Photograph by A.J. Desbarats. NRCan Photo Database number 2020-614.

Figure 7: Typical view of the slag disposal area. The slag occurs in large chunks of varying size, texture, and degree of weathering. Photograph by A.J. Desbarats. NRCan Photo Database number 2020-615.

3.2 Radiometric survey

Radiometric measurements in the slag disposal area were conducted using a Radiation Solutions Inc. RS-230 BGO Super-SPEC® handheld gamma-ray spectrometer. In order to obtain a representative and unbiased survey of slag radioactivity, a longitudinal transect through the disposal area was marked by measuring tape (Figure 8). Measurements were spaced every 2 m along the profile for a total of 46 stations. Radiometric assays (% K, counts per minute, dose rate, ppm of U and Th equivalents) at each station were performed using a 120 second sampling time with the probe in contact with the sampled material. Most measurements were made on slag although some were made on a patch of waste rock fill where slag was absent.

Figure 8: Spectral radiometric survey along a longitudinal profile of the slag disposal area. Spectrometer measurements were performed every 2 m along the yellow measuring tape shown in the photo above. Photograph by J.B. Percival. NRCan Photo Database number 2020-616.

3.3 Field-scale slag leach test cells and leachate sampling

Field-scale slag leach test cells (Figure 9) were constructed out of triple-washed 220 L (45 gal.) food-grade HDPE barrels mounted on a wooden palette. A tap line at the base of each barrel leads to a 22 L collection bucket made of food-grade plastic. One barrel (Barrel #1) was left empty and used as a control to collect precipitation. The three other barrels (Barrels #2, 3, 4) were filled with gravel- to cobble-sized fragments of weathered slag (Figure 10). Part way through the leach experiment, 20 L of mine tailings were added to barrel #4 in order to investigate the chemistry of

leachate from co-disposed slag and tailings. Unfortunately, this leach cell failed after the next sampling event. The cause of failure is not known but may be due to an inaccessible detachment or blockage of the tap line.

The leach experiment was started on June 14, 2017 and was concluded on November 5, 2018 after 6 sampling events. Sampling was carried out in July, September, and November of 2017, and in May, September, and November of 2018. A total of 22 leachate samples were obtained over the duration of the experiment including 6 controls.

Accumulated leachate (or precipitation) was collected in covered plastic buckets and sampled periodically. Leachate pH was measured using a Denver Instruments® U-10 meter calibrated daily over the 7-10 range. Specific conductance was measured using an Oakton® CON 11 meter calibrated daily for the 0 to 1413 µS/cm range. Temperature was measured using both these instruments.

Leachate (or precipitation) was sampled directly from collection buckets using all-plastic 50 mL Norm-Ject® syringes triple-rinsed in the water to be sampled. Unfiltered samples for (total) cations were collected in triple-rinsed 60 mL HDPE narrow-mouth bottles (Nalgene® 2002-0002). Filtered (Millipore® Sterivex™ 0.45 µm) samples for anions and cations were collected in 60 mL HDPE narrow-mouth bottles triple-rinsed with filtered water to be sampled. Bottles for cation samples were acidified each evening at the hotel room to pH <2 by adding 0.5 mL of 8 N ultrapure nitric acid. Duplicate water samples were collected at every tenth sample site, and sample blanks were prepared once per field campaign. Samples were stored at 4°C in a hotel room refrigerator pending return to Ottawa.

a)

b)

Figure 9: Two views of the field-scale leach test cells constructed on site adjacent to the slag disposal area. Three barrels are filled with slag and one barrel is left empty to be used as a control for recovering precipitation. Photographs by A.J. Desbarats. NRCan Photo Database numbers a) 2020-617 and b) 2020-618.

a)

b)

Figure 10: Top views of the leach test barrels. The slag consists of weathered gravel (1 cm) to cobble-sized (12 cm) material with a vesicular texture. The card is 8 cm across. Photographs by A.J. Desbarats. NRCan Photo Database numbers a) 2020-619 and b) 2020-620.

3.4 Laboratory Methods

Leachate chemistry

All leachate samples were analyzed at the Inorganic Geochemical Research Laboratory of the Geological Survey of Canada in Ottawa. Analyses of major elements were performed by Inductively Coupled Plasma - Atomic Emission Spectroscopy (ICP-AES) using a Perkin-Elmer 3000 DV. Analyses of trace elements were performed using Inductively Coupled Plasma - Mass Spectrometry (ICP-MS) with a Thermo Corporation X-7 Series II. Determinations of anion concentrations were made with a Dionex DX-600 ion chromatograph using an AS-18 column and gradient elution. Alkalinities were determined using a PC-Titrate System. Element suites analyzed by each method and their corresponding detection limits are listed in Table 3. Samples were not analyzed for radioactive decay products of ^{238}U and ^{232}Th, including radon, nor were they analyzed for microbiological parameters. For each sample batch, analyses were performed on one or more certified standards of known concentrations. Analytical results for field blanks from each trip were below detection limits for all elements. Detection limits are shown in Table 3. Charge balance errors varied between -16.4 % and 7.0 % with a mean value of 1.1 %. The large error of -16.4 % was associated with a single sample of very dilute rainwater with a specific conductance of 14.3 µS/cm. All other errors were within +/- 7 %.

Slag geochemistry

Samples of slag were analyzed by Bureau Veritas Commodities Canada Ltd. (formerly Acme Labs) at their Vancouver laboratory. Bulk analyses were made using lithium borate fusion with Inductively Coupled Plasma - Emission Spectroscopy (ICP-ES) for whole rock analyses and minor elements, and Inductively Coupled Plasma - Mass Spectrometry (ICP-MS) for trace elements.

Slag radiochemistry

Radioelements were analyzed at the Saskatchewan Research Council Environmental Analytical Laboratories in Saskatoon.

Table 3: Analytical methods and corresponding detection limits for elements analyzed.

ICP-MS Element Suite * lower detection limit in µg/L shown in brackets			
Li (0.02)*	Be (0.005)	B (0.5)	Al (2)
Ti (0.5)	V (0.1)	Cr (0.1)	Mn (0.1)
Co (0.05)	Ni (0.2)	Cu (0.1)	Zn (0.5)
Ga (0.01)	Ge (0.02)	As (0.1)	Se (0.1)
Rb (0.05)	Sr (0.5)	Y (0.01)	Zr (0.05)
Nb (0.01)	Mo (0.05)	Ag (0.005)	Cd (0.02)
In (0.01)	Sn (0.01)	Sb (0.01)	Te (0.02)
Cs (0.01)	Ba (0.2)	La (0.01)	Ce (0.01)
Pr (0.005)	Nd (0.005)	Sm (0.005)	Eu (0.005)
Tb (0.005)	Gd (0.005)	Dy (0.005)	Ho (0.005)
Er (0.005)	Tm (0.005)	Yb (0.005)	Lu (0.005)
Hf (0.01)	Ta (0.01)	W (0.02)	Re (0.005)
Tl (0.005)	Pb (0.01)	Th (0.02)	U (0.005)

ICP-AES Element Suite * lower detection limit in mg/L shown in brackets			
Br (0.05)*	Ca (0.02)	Cl (0.1)	Fe (0.005)
K (0.05)	Mg (0.005)	Na (0.05)	P (0.05)
S (0.05)	Sc (0.001)	Si (0.02)	

IC Element Suite * lower detection limit in mg/L shown in brackets			
F (0.01)*	Cl (0.01)	SO_4 (0.02)	Br (0.02)
NO_3 (0.02)	PO_4 (0.02)		

4. RESULTS

4.1 Physical Description of the Slag

Molten slag from the ferroniobium conversion process was poured into circular pits and cooled to form large "buttons" approximately 1.5 m in diameter and 0.4 m thick (Figure 6). However, after disposal on the site, few of these buttons remained intact. They have since been exposed to approximately 45 years of physical (freeze-thaw) and chemical weathering. Typically, the upper surface of the buttons is tan to reddish-brown with a ropy lava-like texture (Figure A-1). Ferroniobium, as metallic blebs, can sometimes be found around the perimeter of the upper surface. Less commonly, the top of the slag button is grey and smooth, with a well-developed polygonal crack pattern (Figures A-2, A-7). In cross-section, the top 0.15 m of the slag is usually very fine-grained and massive with large horizontal vugs (Figure A-3). Vertical cracks within this layer, sometimes marked by white alteration minerals (Figures 8, A-5, A-6, A-7), form the polygonal pattern seen on the upper surface. This massive layer transitions downward to highly vesicular or sometimes sponge-like material (Figure A-4, A-5). The zonation may reflect more rapid cooling of the top of the slag buttons (Figure 6). Throughout the disposal area, the appearance of the slag is quite variable. Typical examples are described below.

The most common form of slag is a dense and vesicular material with pervasive cracks (Figures A-8, A-9, A-10). The groundmass is dark grey and very fine-grained, with a sugary appearance. The vesicles are lined or completely filled with crystals of a white mineral tentatively identified as gibbsite. Some surfaces of this material (Figure A-10) exhibit a 1 mm thick reddish-brown rind with a ropy texture and sand-paper roughness. This may represent foundry sand fused to the surface of the slag. This type of slag is highly weathered, sometimes to the point of being crumbly (Figure A-8). Because it is abundant and easily broken by hammer, the vesicular material was used selectively to fill the leach test barrels (Figure 10).

Massive slag (Figure A-11) is relatively common on the site. This material is grey-green, dense, and very fine-grained. It is very tough and difficult to break with a hammer or drill with a diamond bit. It usually appears unaltered.

Spongy slag (Figure A-12) is encountered less frequently. It is grey-green, though sometimes black, with a sugary matrix and a sponge-like texture. It shows little apparent sign of weathering.

Glassy slag (Figure A-13) is fairly rare. It is a dense, black, obsidian-like material showing little sign of alteration. Some surfaces appear to be coated with fused foundry sand.

4.2 Mineralogy

The mineral phases forming the ferroniobium slag, together with their compositions and stabilities, are key factors controlling the mobilization of trace elements during weathering processes. This section provides a preliminary summary of mineralogical observations pending completion of a detailed report on the mineralogy of the different mine wastes at the SLC site (J. B. Percival, personal communication). Balkwill-Tweedie (2020) provides a detailed mineralogical analysis of primary and secondary phases based on slag zonation (top, middle, and bottom).

Minerals identified in slag samples by bulk X-ray diffraction are listed in Table 4 along with their ideal compositions. A number of these minerals such as grossite, hibonite, taenite, and perovskite are high-temperature phases typically found in meteorites. The compositions reflect the feedstock of the aluminothermic conversion process, including lime and aluminum powder. The silica is derived from silicate minerals (biotite, pyroxene) in the original pyrochlore concentrate and from foundry sand. Detailed compositions of the slag minerals are not yet available; however, the previous work of Mitchell and Mariano (2016) has shown that trace elements from the pyrochlore, including U, Th, and REEs, are redistributed among the slag mineral hosts.

Table 4: Minerals identified in slag samples from the SLC Mine, Oka, Quebec.

Mineral	Abbreviation	Ideal Formula
Silicates		
Bredigite	Bdg	$Ca_7Mg(SiO_4)_4$
Cristobalite	Crs	SiO_2
Larnite	Lrn	Ca_2SiO_4
Plagioclase feldspar	Pl	$Ca(Al_2Si_2O_8)$
Quartz	Qtz	SiO_2
Carbonates		
Tunisite	Tun	$NaCa_2Al_4(CO_3)_4(OH)_8Cl$
Oxides		
ß-alumina	ß-Al	Al_2O_3
Columbite	Col	$Fe^{2+}Nb_2O_6$ - $Mn^{2+}Nb_2O_6$
Grossite	Gst	$CaAl_4O_7$
Hibonite	Hbn	$CaAl_{12}O_{19}$
Perovskite	Prv	$CaTiO_3$
Uraninite	Urn	UO_2
Hydroxides		
Gibbsite	Gbs	$Al(OH)_3$
Metals		
Taenite	Tae	(Fe,Ni)
Ferroniobium	FeNb	FeNb

Semi-quantitative mineral modal abundances for three slag specimens are presented in Table 5. Sample PSA15-SL01 is unusual in that the crystalline phases consist of silicate minerals although approximately 35% of the sample is X-ray amorphous. This sample probably represents slag hybridized with foundry sand. The cristobalite may have resulted from heating of the sand as the melt was poured into molds. Since cristobalite is metastable at ambient temperatures, it may be slowly converting to quartz.

The other two samples are more typical of SLC slag in that they contain abundant high-temperature minerals. Sample PSA15-SL02 is composed of hibonite (27 %) and minor columbite (10 %) with secondary gibbsite (14 %) from weathering. The sample also contains minor to trace amounts of larnite, grossite, uraninite, perovskite, ß-alumina, cristobalite, and bredigite. Amorphous material (glass) represents 23% of the sample weight. Sample PSA15-SL03 is composed of abundant perovskite (31 %), subordinate grossite (18 %), with minor hibonite, columbite, uraninite and larnite. The sample contains minor to trace taenite, tunisite, gibbsite, and cristobalite. Amorphous material represents 19% of the sample weight.

Table 5: Semi-quantitative mineralogy by XRD analyses for slag samples from the SLC Mine, Oka, Quebec. The compositions represent weight % of the crystalline phases.

Mineral Groups	Minerals	PSA15-SL01	PSA15-SL02	PSA15-SL03
Silicates	Qtz	60		
	Crs	36	5	1
	Pl	4		
	Bdg		5	
	Lrn		9	7
Carbonates	Tun		4	4
Oxides	ß-Al		6	
	Col		10	11
	Gst		7	18
	Hbn		27	12
	Prv		6	31
	Urn		7	9
Hydroxides	Gbs		14	2
Metals	Tae			5
% Crystallinity	% XL	65	77	81

ß-Al: beta-Alumina; Bdg: Bredigite; Col: Columbite; Crs: Cristobalite; Gbs: Gibbsite; Gst: Grossite; Hbn: Hibonite; Lrn: Larnite; Pl: Plagioclase Feldspar; Prv: Perovskite; Qtz: Quartz; Tae: Taenite; Tun: Tunisite; Urn: Uraninite

4.3 Geochemistry and Radiochemistry

Geochemical (Table 6) and radiological (Table 7) analyses were performed on the three samples of slag described in section 4.2 and on one archived sample of pyrochlore concentrate from the SLC mine. Comparisons between slag and concentrate compositions illustrate elemental gains and losses associated with the ferroniobium conversion process.

Concentrate from the SLC mill consisted of pyrochlore (92-98 %), perovskite (tr-5 %), biotite (tr-5 %), pyroxene (tr-5 %), monticellite (tr-3 %), tremolite (tr-1 %), and trace amounts of sulfides, magnetite and calcite (Gold and Vallée, 1969). Sample PNA15-11 (Table 6) appears typical of SLC concentrate (Table V, Carbonneau and Caron, 1965). With an Nb_2O_5 content of 52 %, it contains less than 1 % Ta_2O_5, less than 4 % SiO_2, between 4 and 6% TiO_2, and less than 0.06 % P. Notably, it also contains significant concentrations of Th, U, Zr and light REE.

Given that pyrochlore concentrate specifications require that SiO_2 not exceed 4 % and that silica is not added to the aluminothermic charge, the high (72 %) SiO_2 content of slag sample PSA15-SL01 is unusual, as noted above. This probably represents hybridization of molten slag with foundry sand. Slag samples PSA15-SL02 and PSA15-SL03 generally have similar major element compositions despite differences in their mineralogy. Both contain approximately 50 % Al_2O_3, 15 % CaO, 5 % TiO_2, and between 5 and 10 % SiO_2. The Al_2O_3 is derived almost entirely from the aluminum powder fueling the conversion. Sample PSA15-SL02 contains notable Fe_2O_3 and Nb_2O_5 indicating the presence of unrecovered ferroniobium or columbite. The trace element compositions of the two slag samples are similar also, and comparable to that of typical concentrate. For example, as shown in Figure 11, the REE signatures of concentrate and slag samples are essentially identical. This provides evidence that trace elements in the pyrochlore concentrate partition into the slag rather than the ferroniobium. Importantly, this illustrates how naturally occurring radioactive material (NORM) found in pyrochlore is enhanced through ore beneficiation and sequestered in the slag through the ferroniobium conversion process. In a typical slag (PSA15-SL03), U and Th concentrations are 1188 and 2492 ppm, respectively (Table 6). For the Oka-1 Niobium ore Certified Reference Material (Steger and Bowman, 1981) used as an analytical standard in this study, the mean U and Th concentrations from duplicate analyses are 29 and 61 ppm, respectively. Thus, the enhancement factor is about 41 for both U and Th concentrations.

Calculated activity concentrations for U-238 range between 4.8 and 27.5 Bq/g in slag compared to a value of 17.6 Bq/g in concentrate (Table 7). The measured activities of daughter products are usually similar to those of U-238, which suggests approximate secular equilibrium. Calculated and measured activity concentrations of U-235 are close, and lower than those of U-238 by approximately the theoretical factor of 21.3. Measured activities on daughter products of U-235 also suggest conditions approaching secular equilibrium. Calculated activity concentrations for Th-232 range between 5.1 and 10.1 Bq/g in slag compared to a value of 6.4 in concentrate. For most daughter products measured activities are close to those of Th-232.

Activity concentrations for the entire U-238, U-235, and Th-232 decay series are summarized in Table 8. Values were calculated assuming secular equilibrium between parent radionuclide and daughter products.

Table 6: Geochemistry of selected pyrochlore concentrate and slag samples.

%	PNA15-11 Concentrate	PSA15-SL01 Slag	PSA15-SL02 Slag	PSA15-SL03 Slag
SiO_2	2.72	71.90	4.57	9.53
Al_2O_3	0.42	13.13	50.12	49.81
Fe_2O_3	2.44	1.16	4.89	0.48
MgO	0.44	0.12	1.44	0.32
CaO	16.16	6.80	13.46	16.23
Na_2O	4.47	0.94	0.61	1.14
K_2O	0.15	0.10	0.32	0.05
TiO_2	5.05	1.76	4.23	6.25
P_2O_5	0.10	0.03	<0.01	<0.01
MnO	0.39	0.04	0.13	0.09
Cr_2O_3	<0.002	0.003	<0.002	<0.002
Nb_2O_5	51.93	0.33	8.32	0.78
LOI	1.10	0.60	1.50	4.20
Sum	85.37	96.91	89.59	88.88
ppm				
Ba	2246	904	1387	833
Sr	4393	1858	3105	3947
Ta	4049	75	1495	1206
Th	1574	1477	1265	2492
U	1424	386	2227	1188
Zr	15266	3881	12299	9150
Y	781	266	751	687
La	9404	1869	7758	7980
Ce	79800	11748	49886	53800
Pr	3174	771	2734	2751
Nd	9239	2190	7578	7862
Sm	1130	311	1028	1042
Eu	308	72	288	256
Gd	808	219	785	839
Tb	65	21	61	63
Dy	291	93	281	264
Ho	36	12	32	32
Er	84	29	79	77
Tm	12	4	11	10
Yb	72	23	66	63
Lu	6	2	6	5

Table 7: Measured activity concentrations in slag and pyrochlore concentrate for daughter products of a) U-238, b) U-235, and c) Th-232

a) U-238

Sample ID	Type	U (ppm)	U-238* activity (Bq/g)	Th-234 activity (Bq/g)	Th-230 activity (Bq/g)	Ra-226 activity (Bq/g)	Pb-214 activity (Bq/g)	Bi-214 activity (Bq/g)	Pb-210 activity (Bq/g)
PSA15-SL01	slag	385.7	4.8	4.6	6	4	4.1	4.2	3.0
PSA15-SL02	slag	2226.6	27.5	19.0	30	26	26.0	25.0	11.0
PSA15-SL03	slag	1187.6	14.7	11.0	15	9	10.0	9.9	4.6
PNA15-11	conc.	1423.8	17.6	6.2	9	12	12.0	12.0	3.4

b) U-235

Sample ID	Type	U (ppm)	U-235* activity (Bq/g)	U-235 activity (Bq/g)	Th-227 activity (Bq/g)	Ra-223 activity (Bq/g)	Rn-219 activity (Bq/g)	Pb-211 activity (Bq/g)
PSA15-SL01	slag	385.7	0.2	0.25	0.12	0.4	0.1	0.2
PSA15-SL02	slag	2226.6	1.3	1.60	1.10	1.4	1.2	3.0
PSA15-SL03	slag	1187.6	0.7	0.90	0.60	0.9	0.4	1.0
PNA15-11	conc.	1423.8	0.8	0.80	0.60	1.0	0.4	2.0

c) Th-232

Sample ID	Type	Th (ppm)	Th-232* activity (Bq/g)	Ac-228 activity (Bq/g)	Pb-212 activity (Bq/g)	Bi-212 activity (Bq/g)	Tl-208 activity (Bq/g)
PSA15-SL01	slag	1477.2	6.0	5.7	5.7	3.8	1.9
PSA15-SL02	slag	1264.9	5.1	5.2	5.2	3.3	1.7
PSA15-SL03	slag	2491.6	10.1	10.0	10.0	6.6	3.2
PNA15-11	conc.	1574.2	6.4	5.4	5.3	3.6	1.8

* Calculated values based on measured U and Th concentrations, 99.28% U-238 in natural uranium and specific activities of 12445 Bq/g, 80476 Bq/g, and 4059 Bq/g for U-238, U-235, and Th-232, respectively.

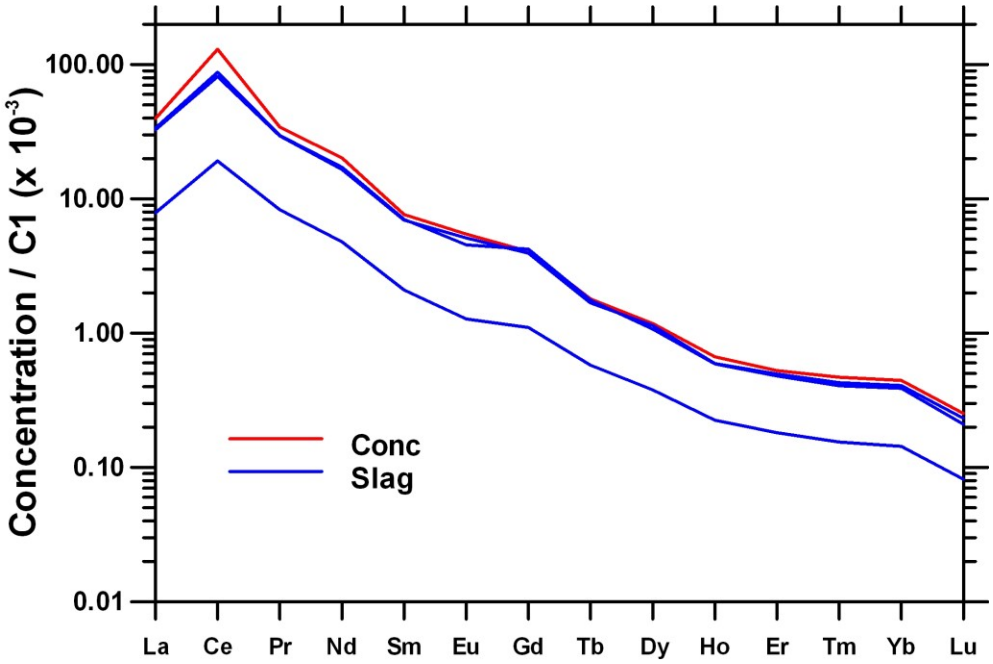

Figure 11: C1-Chondrite-normalized REE patterns for concentrate and slag samples of Table 6. C1-chondrite REE abundances are from McDonough and Sun (1995).

Table 8: Calculated total activity concentrations for the decay series of U-238, U-235, and Th-232 assuming secular equilibrium.

Sample ID	Type	U-238 decay series activity conc.	U-235 decay series activity conc.	Th-232 decay series activity conc.	Total (U + Th) activity conc.
		(Bq/g)	(Bq/g)	(Bq/g)	(Bq/g)
PSA15-SL01	slag	66.7	2.4	65.9	135.0
PSA15-SL02	slag	385.1	14.2	56.5	455.8
PSA15-SL03	slag	205.4	7.6	111.2	324.2
PNA15-11	conc.	246.3	9.1	70.3	325.7

4.4 Radiometric survey of the slag disposal area

A radiometric survey of the slag disposal area was conducted in order to obtain a more representative characterization of slag radioactivity and radioelement concentrations. The survey was conducted along a longitudinal transect of the disposal area with measurement stations every 2 m. A total of 46 radiometric assays (% K, ppm of U and Th equivalents) were performed including 37 on slag material and 9 on barren fill.

The profile of equivalent U concentrations (Figure 12) across the disposal area shows that values in slag are relatively uniform and close to 1000 ppm. The profile of equivalent Th concentrations (Figure 12) is much more erratic with spikes as high as 5000 ppm. The average Th concentration is higher also. The corresponding dose rates reported by the instrument are shown in Figure 13. Profiles of activity concentrations for the U and Th decay chains (Figure 14) were calculated from the radiometric U and Th assays, respectively, and are therefore similar in character. Because of uranium's greater specific activity, the total activity concentration of slag is dominated by its U content even though its Th content is usually higher. Summary statistics of the slag survey (Table 9) are consistent with results in Tables 7 and 8. For the three slag samples, the average activity concentrations from the U and Th decay chains are 227 Bq/g and 78 Bq/g, respectively, compared to 189 Bq/g and 95 Bq/g for the survey, respectively.

Table 9: Summary statistics for radiometric survey results (slag material only).

	Uranium equivalent (ppm)	Thorium equivalent (ppm)	U-238 + U-235 activity conc. (Bq/g)	Th-232 activity conc. (Bq/g)	Total activity conc. (Bq/g)
N	37	37	37	37	37
Minimum	455	607	81.6	27.1	126.3
Maximum	1616	5069	289.8	226.3	417.4
Median	1069	2101	191.7	93.8	303.8
Mean	1051	2133	188.6	95.2	283.8
Stand. Dev.	238	848	42.7	37.8	69.9

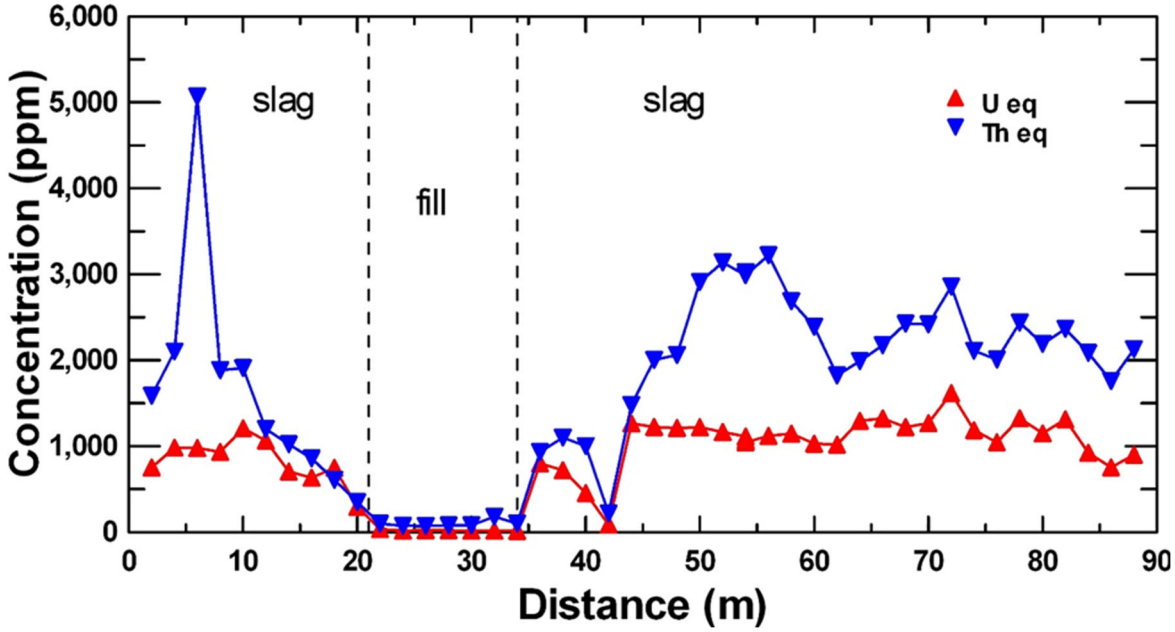

Figure 12: Spectral radiometric survey of the slag disposal area showing concentrations of U and Th equivalents on the longitudinal transect.

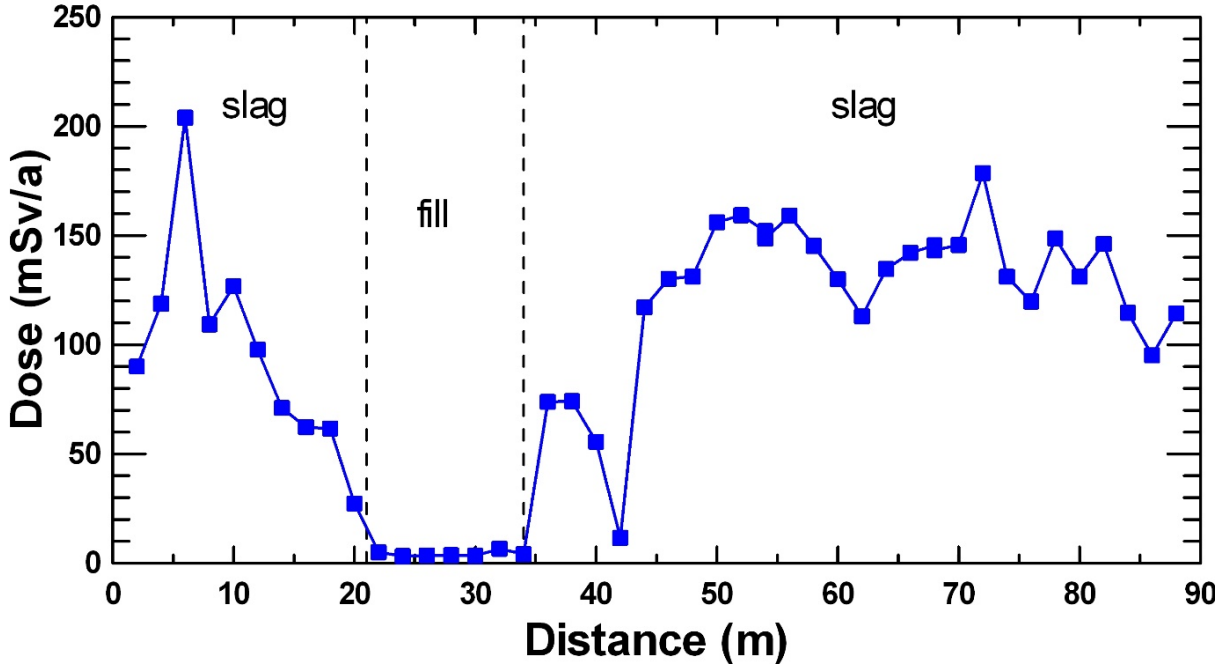

Figure 13: Spectral radiometric survey of the slag disposal area showing calculated dose rate along the longitudinal transect.

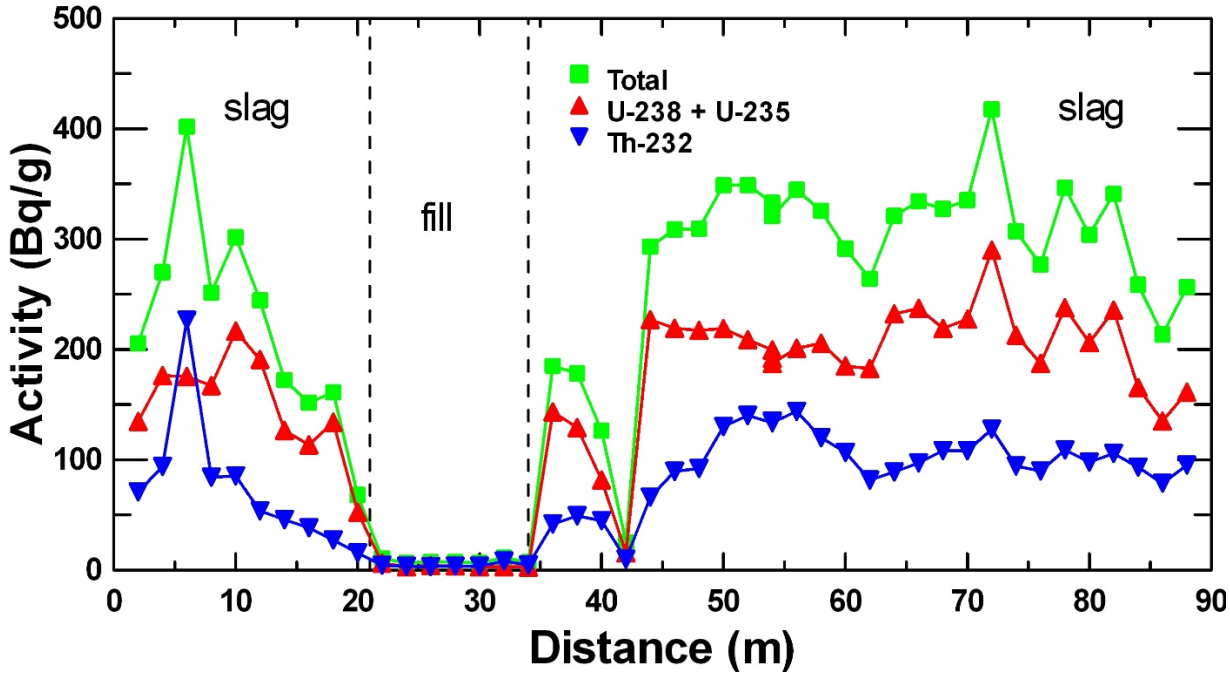

Figure 14: Spectral radiometric survey of the slag disposal area showing total activity concentrations of U and Th decay series along the longitudinal transect.

4.5 Slag Leachate chemistry

The evolution of leachate chemistry during the experiment is expressed as a function of cumulative flush volume measured in the control barrel. Recovered precipitation in the control barrel is in reasonable agreement with precipitation recorded at the nearby Oka weather station. Volumes of leachate recovered in slag barrels are somewhat less than volumes of water recovered in the control barrel due to moisture retention on slag particles and resulting losses to evaporation. Based on slag granulometry and barrel dimensions, the estimated porosity and pore volume of the barrels are 0.20 and 40 L, respectively. Over the duration of the leach experiment, the slag barrels were flushed by approximately 85 L of precipitation or about 2 pore volumes. Unless otherwise indicated concentrations are for filtered (< 0.45 µm) samples.

Field Parameters

The specific conductance of slag leachate is relatively high and varies between 1190 and 3280 µS/cm (Figure 15). Values increased initially during the summer of 2017 then decreased over the following fall and winter. Values increased again in the fall of 2018. Most chemical parameters follow a similar pattern. Steady-state leachate concentrations do not appear to have been reached

during the course of the experiment. Given the pervasively cracked and vesicular nature of the slag (Figures 10, A-8, A-9), it is likely that physical weathering, such as freeze-thaw action, is ongoing. This increases the slag surface area and continuously exposes fresh material to leaching.

The pH of leachate is generally elevated but stable in the range of 8.8 to 9.4 (Figure 16). However, the pH of barrel #4 leachate dropped sharply to 7.8 following the addition of calcite-rich mine tailings after the third sampling event in the fall of 2017.

Major Cations and Anions

The dominant cation in the leachate is Na from the sodium chlorate ($NaClO_3$) used as a chemical oxygen generator in the ferroniobium conversion process. The evolution of Na concentrations mirrors that of specific conductance and values range between 287 and 875 mg/L (Figure 17). Concentrations of Ca and Mg are generally very low and stable throughout the experiment (Figure 18 and 19). However, these figures also show the drastic effects of adding calcite-rich tailings to barrel #4. Concentrations of K, likely derived from biotite in the pyrochlore concentrate, follow a similar pattern to those of Na (Figure 20).

Leachate alkalinities are elevated and reach as high as 1445 mg/L CaCO3 equivalent or 29 meq/L (Figure 21). The evolution of alkalinities follows a pattern similar to those of the dominant cation (Na) and specific conductance. Sulfate concentrations are generally low and stable throughout the experiment (Figure 22). Sulfide minerals in the pyrochlore concentrate are the likely source of sulfate. However, it can be seen that tailings added to barrel #4 greatly increased the sulfate concentration of the leachate. Nitrate concentrations (Figure 23) are high but follow the same evolution pattern as Na. The source of nitrate is unclear. Chloride (Cl) concentrations are also fairly high (Figure 24). The source of Cl, like that of Na, is most likely the sodium chlorate used in the ferroniobium conversion process. Fluoride concentrations are very high, reaching 46 mg/L (Figure 25). They follow the same pattern as those of Na. The main source of F is likely to be the fluorite flux used in the ferroniobium conversion process although some F is hosted in pyrochlore itself. Concentrations of phosphate are at or near the detection limit (0.02 mg/L) throughout the experiment and are not shown. Dissolved organic carbon (DOC) in the slag leachate is as high as 140 mg/L initially, then decreases gradually before reaching a plateau between 10 and 20 mg/L (Figure 26). DOC concentrations in the control barrel are below 5 mg/L. The source of DOC in the slag barrels is unclear. It may represent an organic coating on slag chunks accumulated over more than 40 years from forest litter.

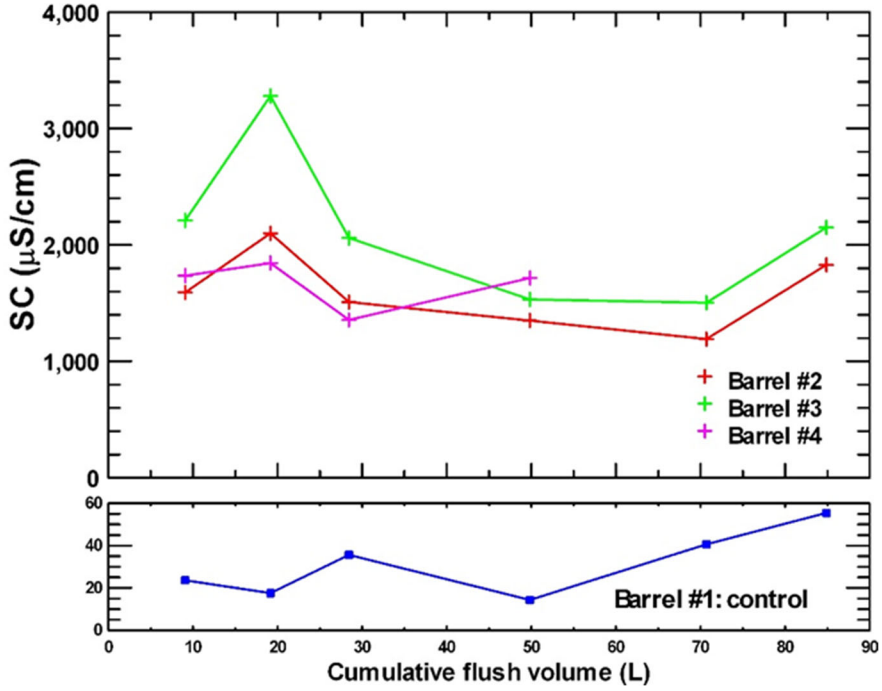

Figure 15: Temporal evolution of leachate chemistry – specific conductance.

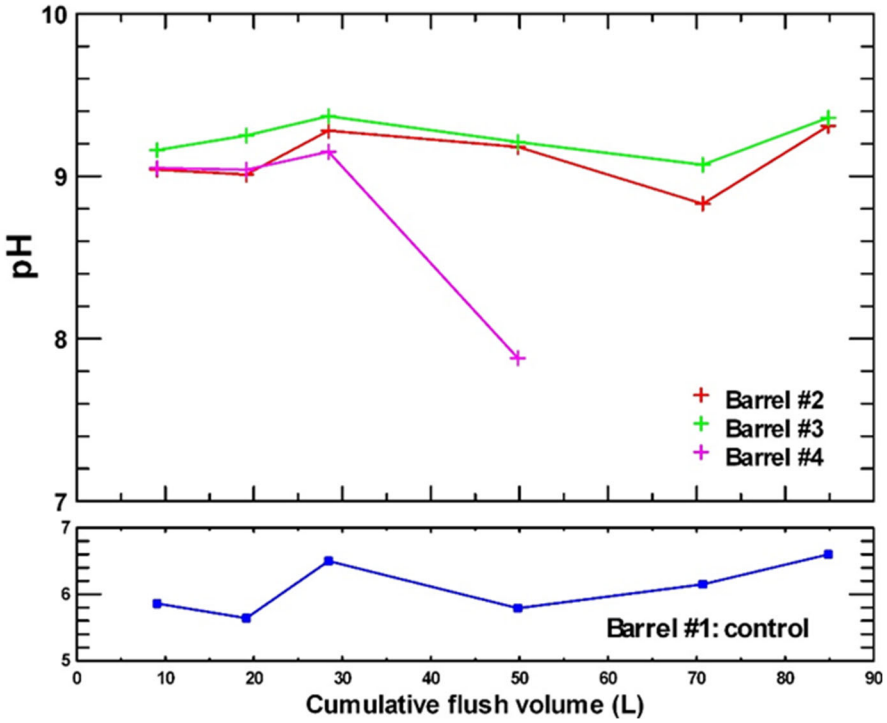

Figure 16: Temporal evolution of leachate chemistry – pH.

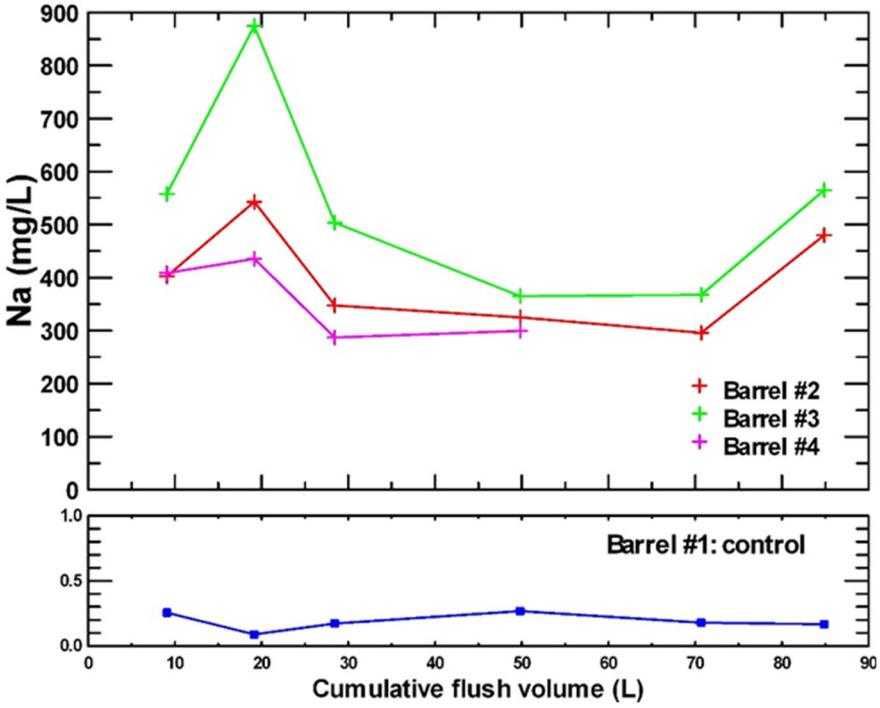

Figure 17: Temporal evolution of leachate chemistry – sodium (Na).

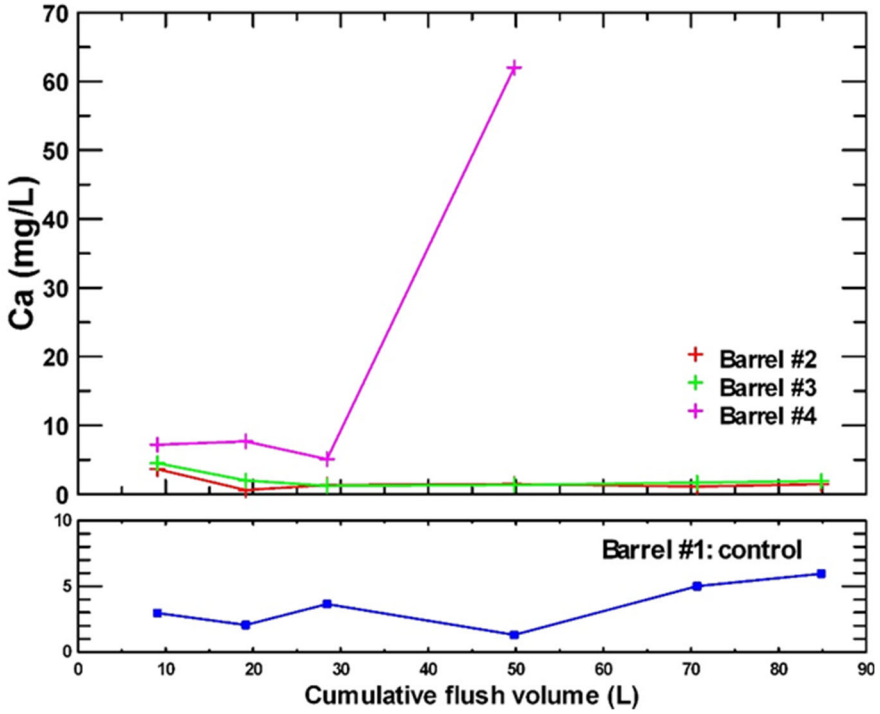

Figure 18: Temporal evolution of leachate chemistry – calcium (Ca).

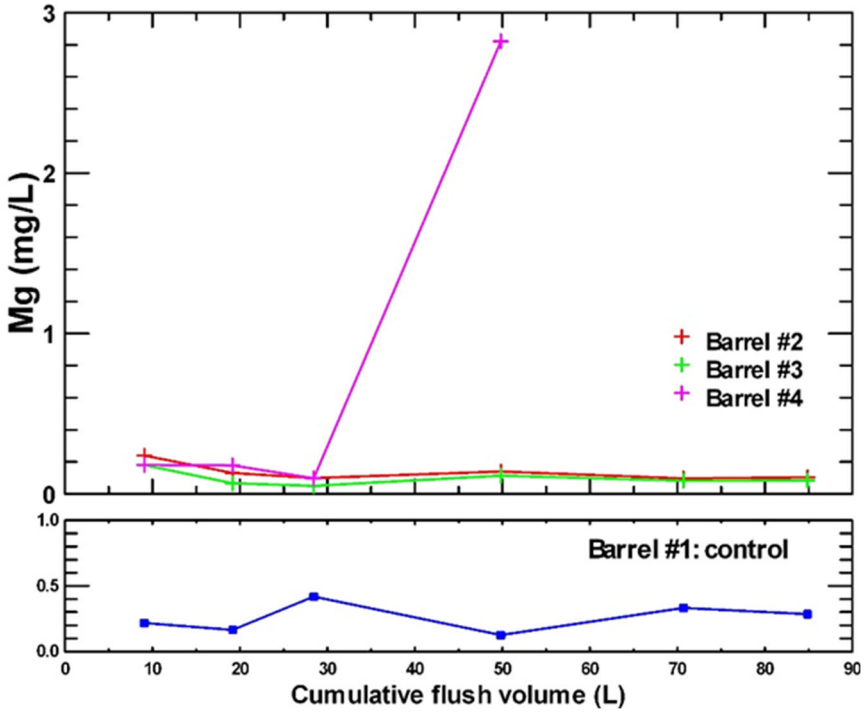

Figure 19: Temporal evolution of leachate chemistry – magnesium (Mg).

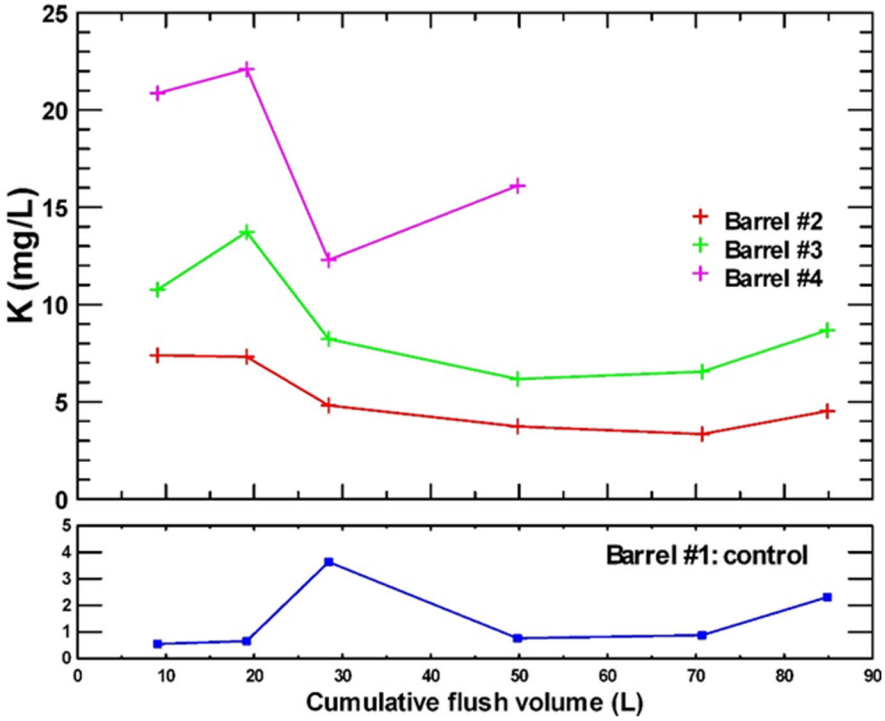

Figure 20: Geochemical evolution of leachate composition – potassium (K).

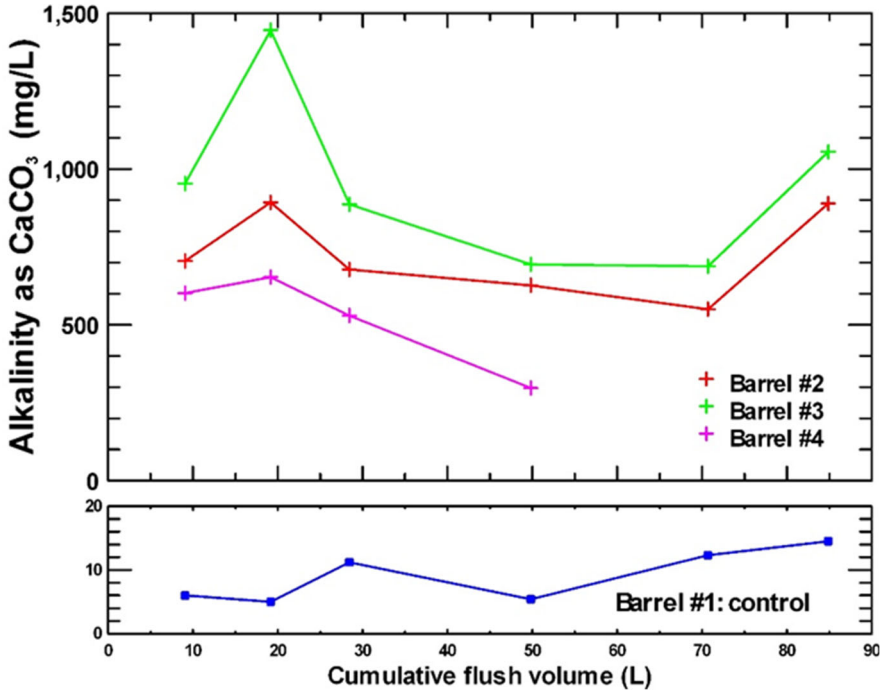

Figure 21: Temporal evolution of leachate chemistry – alkalinity as $CaCO_3$.

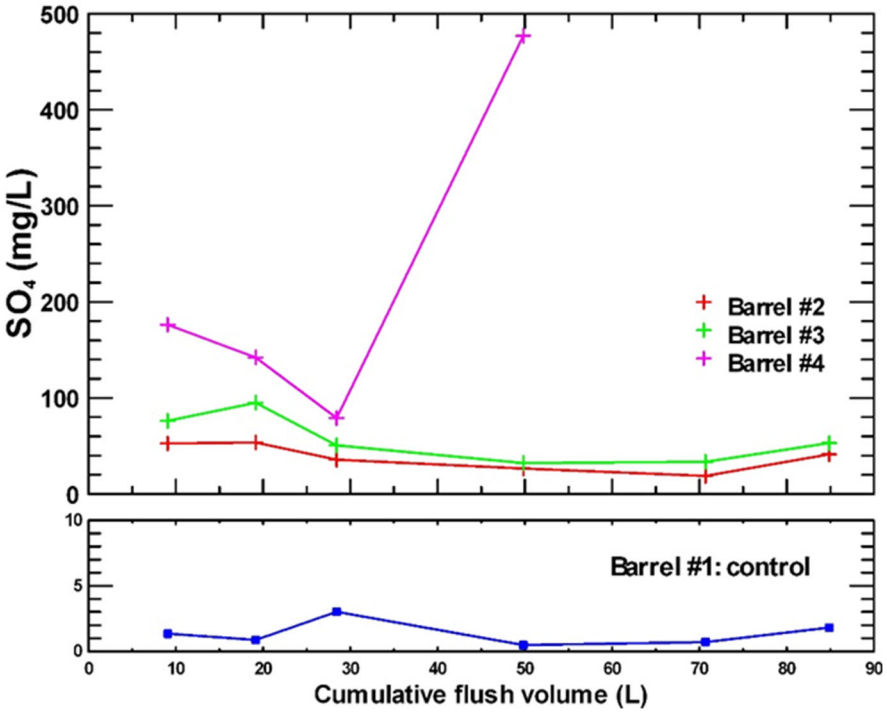

Figure 22: Temporal evolution of leachate chemistry – sulfate (SO_4).

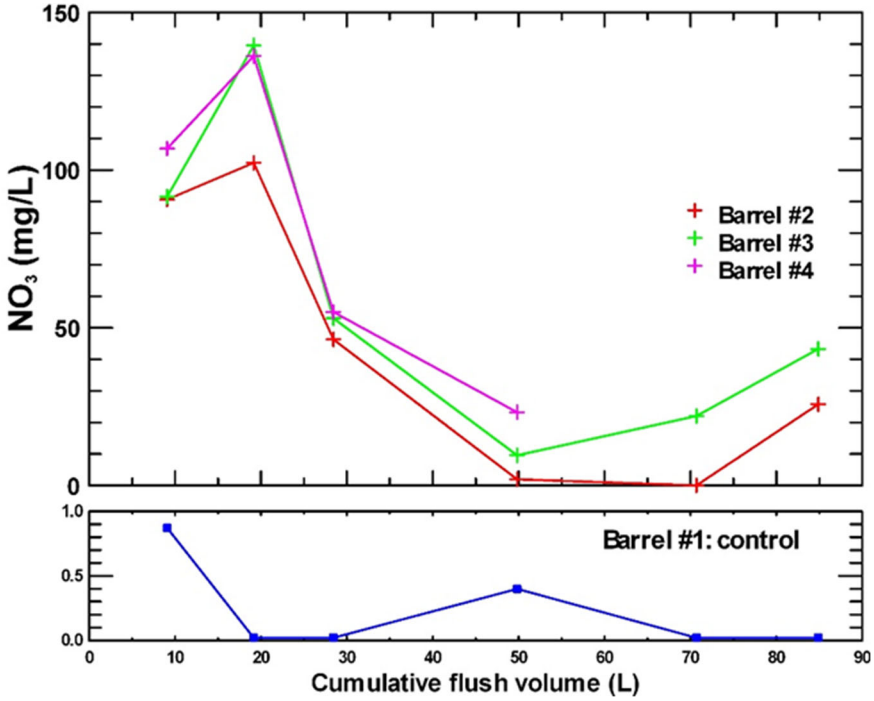

Figure 23: Temporal evolution of leachate chemistry – nitrate (NO_3).

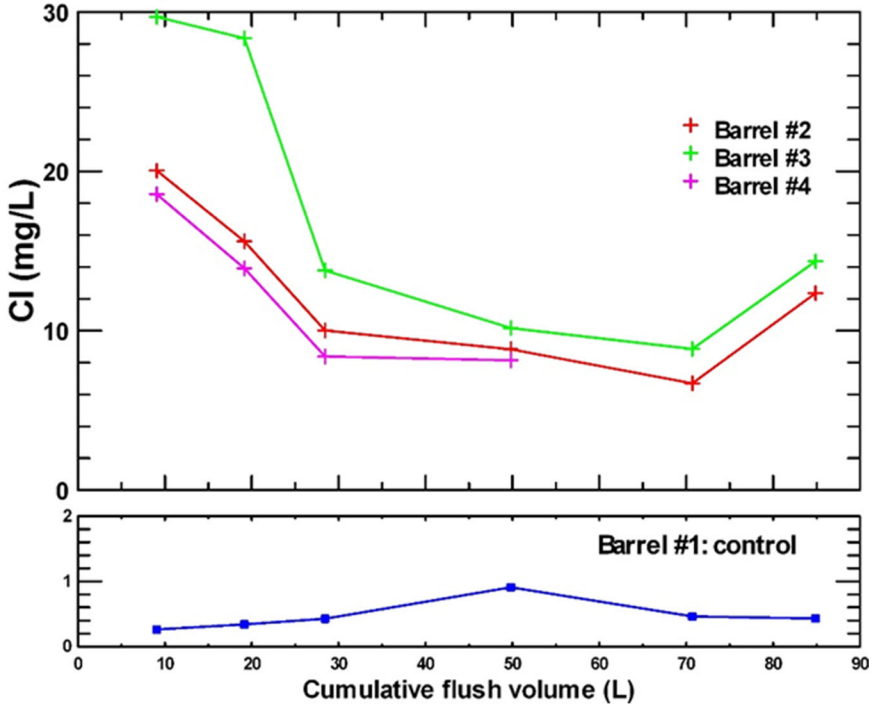

Figure 24: Temporal evolution of leachate chemistry – chloride (Cl).

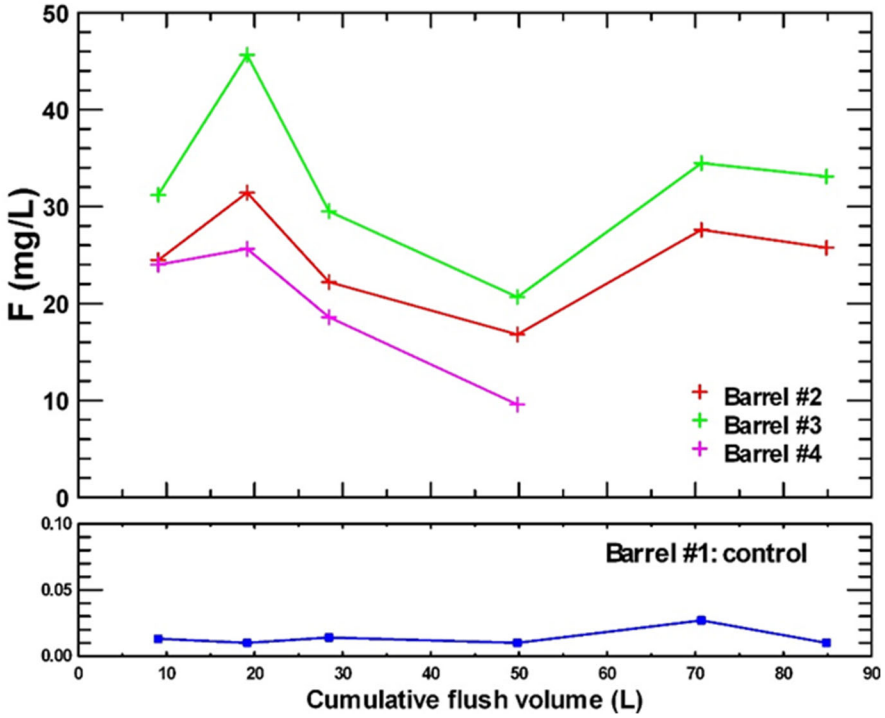

Figure 25: Temporal evolution of leachate chemistry – fluoride (F).

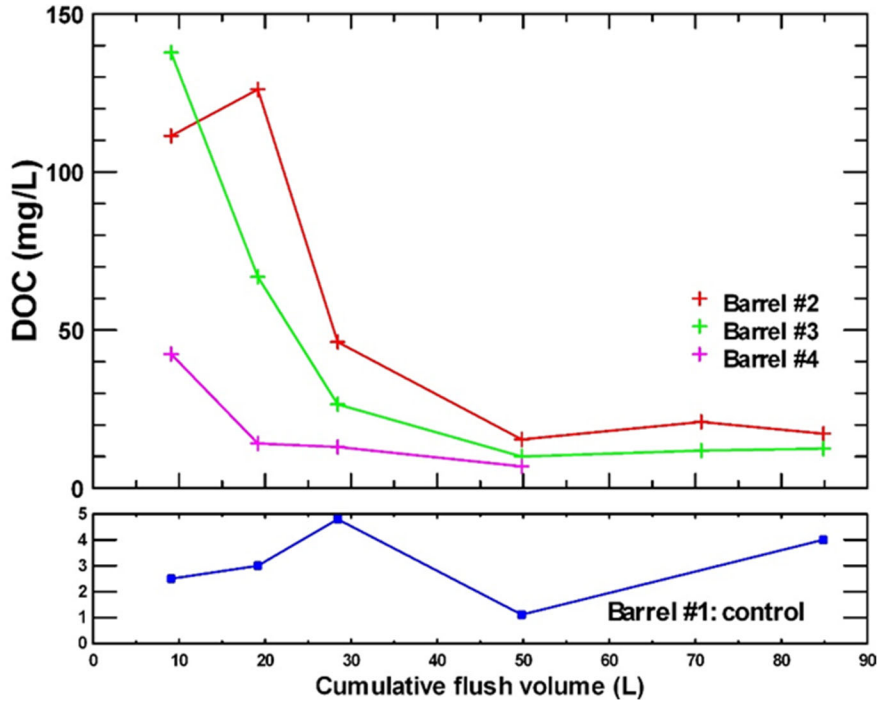

Figure 26: Temporal evolution of leachate chemistry – dissolved organic carbon (DOC).

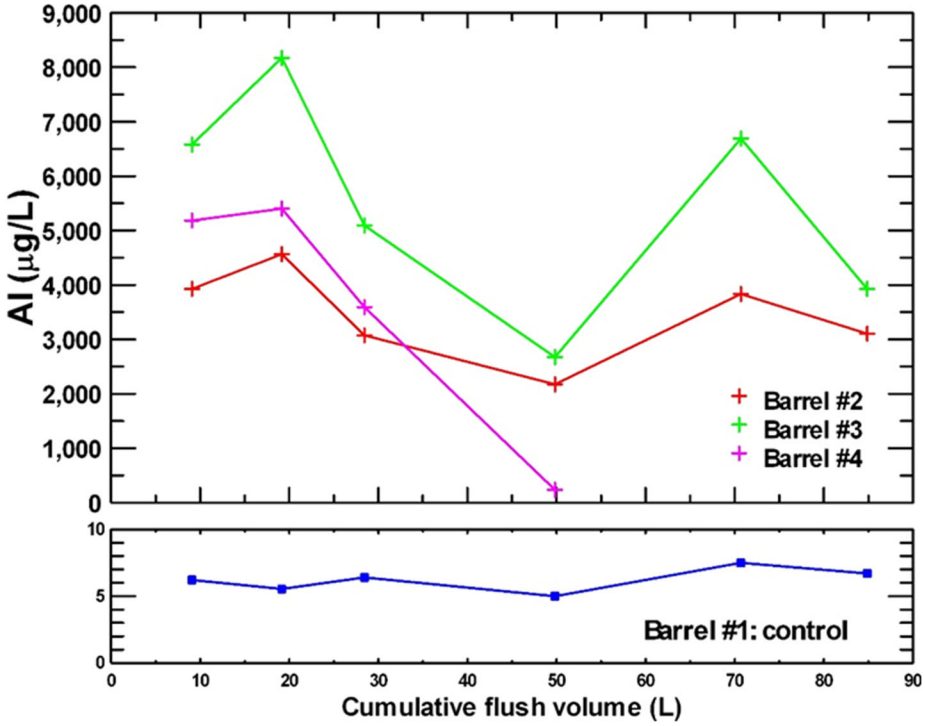

Figure 27: Temporal evolution of leachate chemistry – aluminum (Al).

Selected trace elements

Aluminum concentrations in slag leachate are extremely high. Values generally exceed 2 mg/L and reach 8.17 mg/L (Figure 27). The pattern of Al evolution follows that of the major dissolved species with the exception of leachate from barrel #4. In this case, the addition of tailings appears to have caused a very sharp decrease in concentration to 0.23 mg/L. The original source of Al is undoubtedly the Al powder used to fuel the aluminothermic reduction process. Niobium concentrations in leachate vary significantly between barrels although they are generally high and may exceed 200 µg/L (Figure 28). Uranium concentrations are moderately high throughout the experiment and range between 16 and 65 µg/L (Figure 29). They follow the usual pattern of evolution. Thorium concentrations in leachate are near or below the analytical detection limits (0.02 or 0.2 µg/L) and results are not shown. Zirconium concentrations vary significantly between barrels and over the duration of the experiment (Figure 30). Values are unusually high and sometimes exceed 30 µg/L.

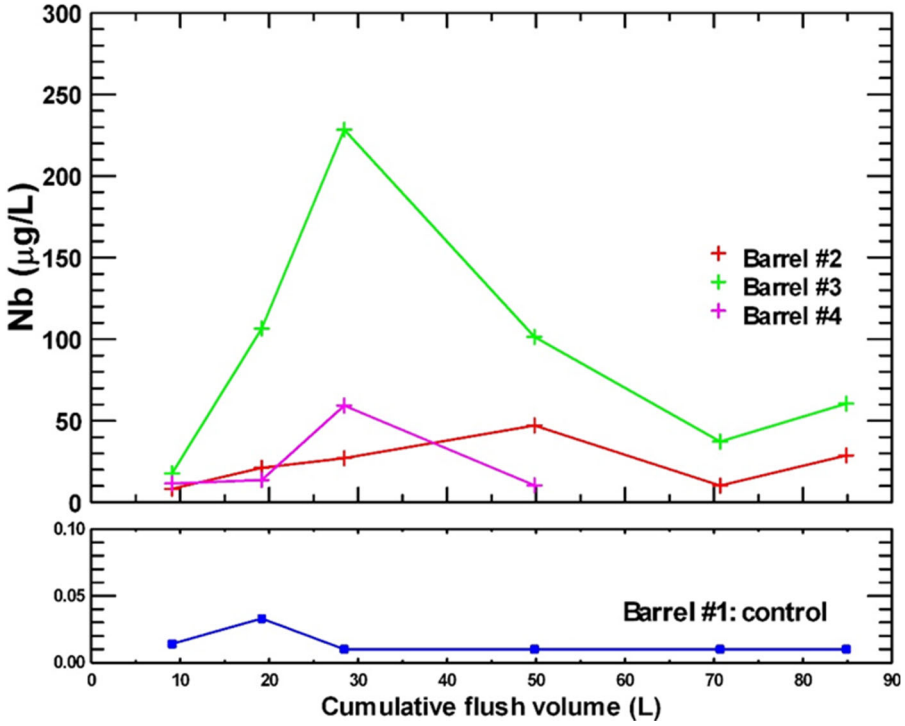

Figure 28: Temporal evolution of leachate chemistry – niobium (Nb).

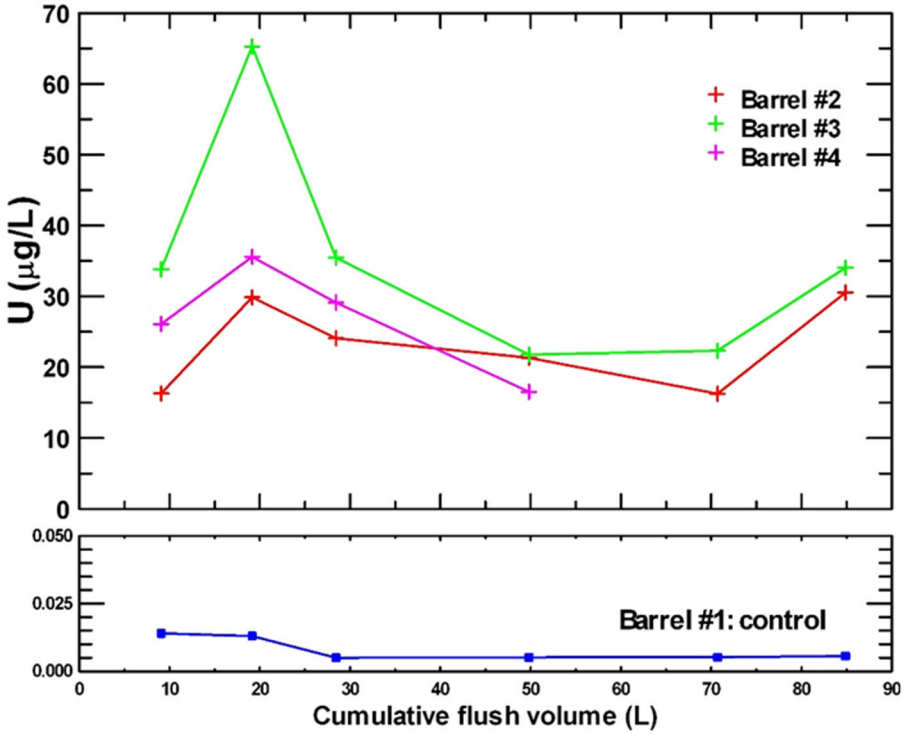

Figure 29: Temporal evolution of leachate chemistry – uranium (U).

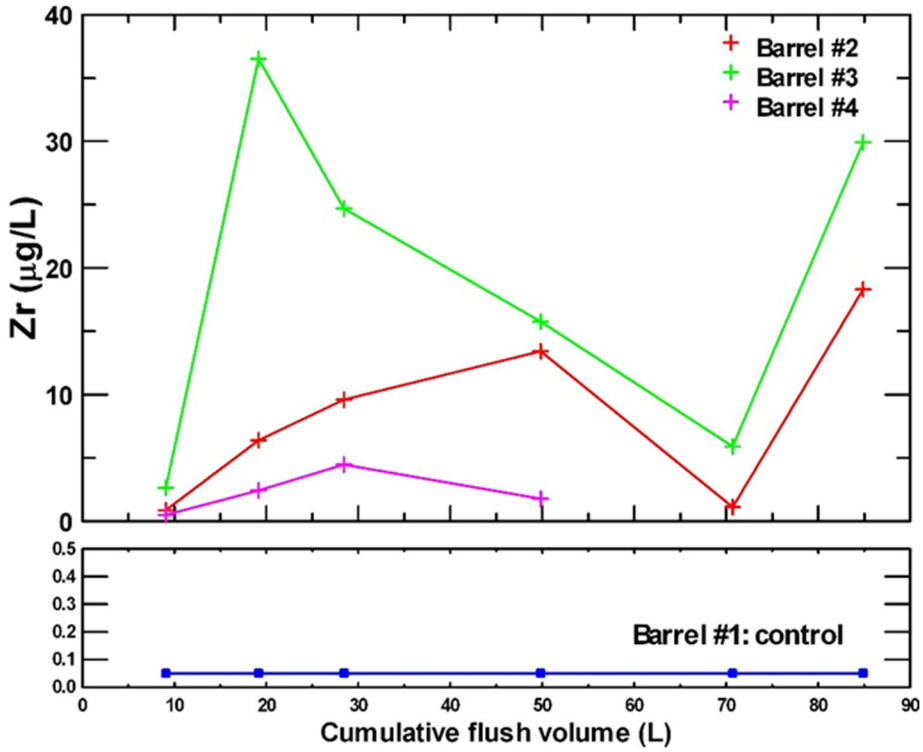

Figure 30: Temporal evolution of leachate chemistry – zirconium (Zr).

5.0 DISCUSSION

5.1 Interpretation of leach experiment results

Source phases of dissolved species

In this study, minerals identified in Oka slag include hibonite, grossite, perovskite, beta-alumina, columbite, uraninite, and gibbsite (Table 4). Non-crystalline (glass) phases were also observed. In their study of Oka slag, Mitchell and Mariano (2016) found that most of the slag consisted of a very fine groundmass of (in order of crystallization) hibonite, beta-alumina, calcium zirconate, REE-Al-Ca-Ti perovskite, and calcium aluminate glass. The rest of the slag was relatively coarse grained and consisted of anorthite crystals set in F-Na-Ce aluminosilicate glass. Based on detailed compositions for the different phases (Mitchell and Mariano, 2016), geochemical cross-plots of concentrations of dissolved species are used here to infer their slag mineral source(s). As they represent compositional data (Aitchison, 1986), concentrations are normalized using a log-ratio transformation with SiO_2 concentrations selected here as the denominator.

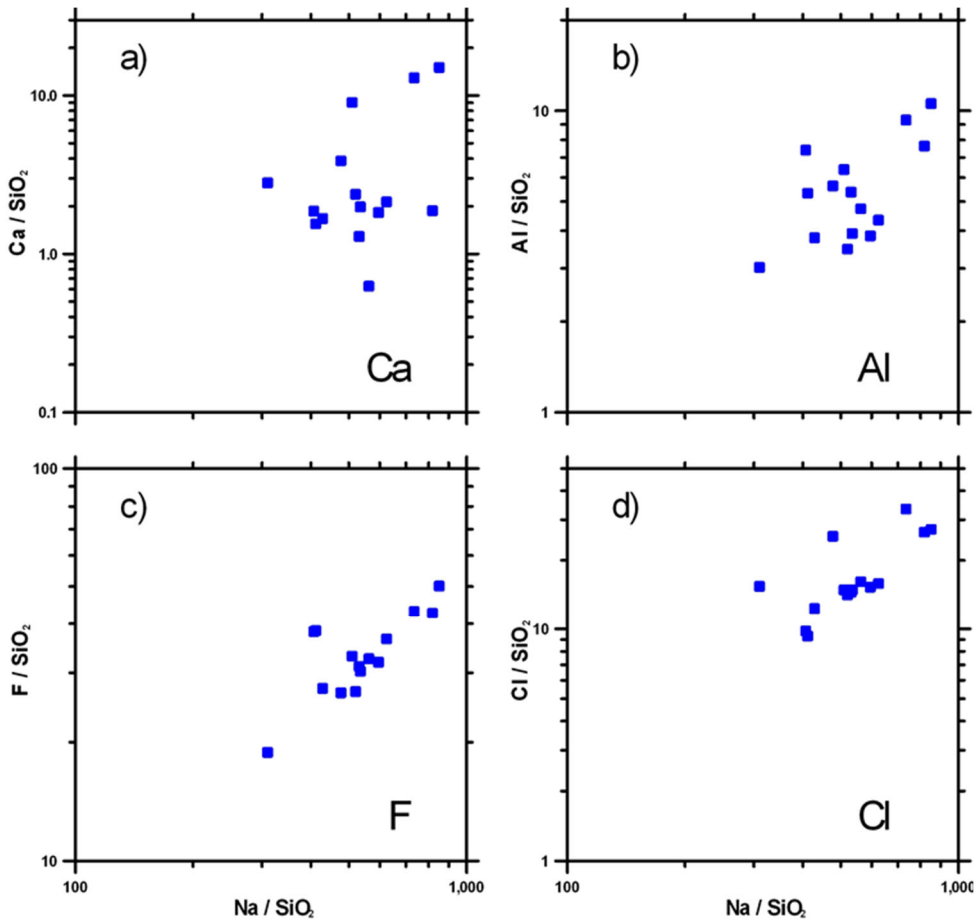

Figure 31: Slag source for major dissolved species: Cross-plots of Na / SiO_2 with a) Ca / SiO_2; b) Al / SiO_2; c) F / SiO_2; d) Cl / SiO_2.

According to Mitchell and Mariano (2016), the final phases to form in Oka slag are calcium aluminate glasses enriched in F, Na, and Ce. These glasses are the main hosts of Na in the slag and they are likely the most leachable phases since Na is by far the most important dissolved cation. Therefore, cross-plots of (normalized) Na concentrations with those of other species should indicate if they are also sourced from the glass phases. Fluoride is strongly correlated with Na, as expected if Na and F are both derived from the glass phases (Figure 31c). Aluminum and Cl also exhibit significant correlations with Na although Ca does not. The Ca is found mainly in crystalline phases, which may be less susceptible to weathering than glass phases.

The anorthite glass was the only phase found by Mitchell and Mariano (2016) to contain S. Strong correlations between (normalized) SO_4, Ca and K concentrations (Figure 32) suggest that secondary alunite ($KAl_3(SO_4)_2(OH)_6$) and possibly gypsum may be forming in the slag barrels during dry spells and dissolving during rainfall events.

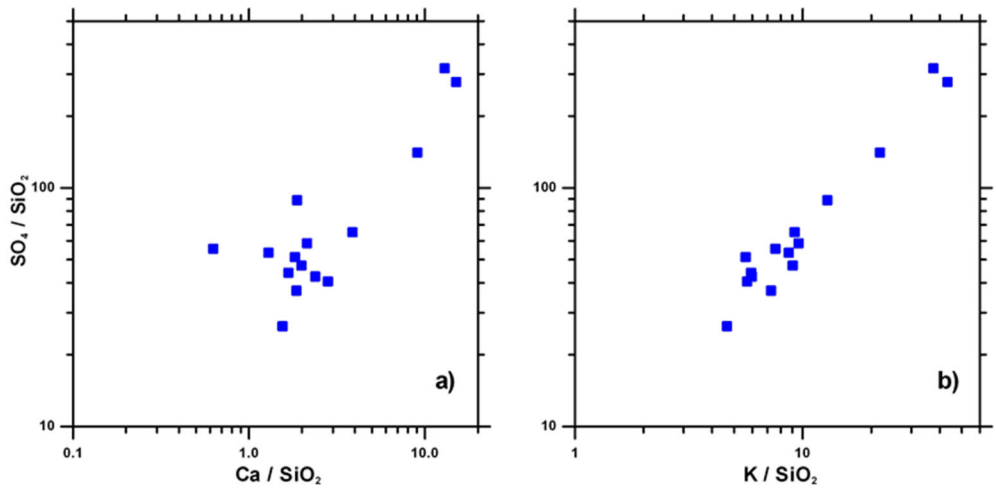

Figure 32: Slag source for major dissolved species: Cross-plots of SO_4 / SiO_2 with a) Ca / SiO_2; b) K / SiO_2.

Cross-plots of normalized Na concentrations versus those of trace elements serve to identify which elements are readily mobilized from the glass phases (Figure 33). Although U, REE, Nb, and Zr are widely distributed among all the phases in the slag, strong correlations with Na suggest that U and Ce in leachate are likely derived from the glasses (Figure 33). Niobium and Zr exhibit weaker correlations with Na suggesting that they may be derived from more than one host. However, trace elements in slag leachate will be derived only from those hosts that are most unstable under ambient low-temperature conditions. Geochemical plots and mineral stability considerations generally suggest that the glass and perovskite (Nesbitt et al., 1981; Lumpkin et al., 2014) phases are the main sources of dissolved species in slag leachate. Most trace elements in the slag are distributed among multiple mineral phases. As noted by Mitchell and Mariano (2016), these phases vary considerably in abundance and in composition. Thus, without further investigations, it is not possible here to conclusively identify source phases for all leachate constituents.

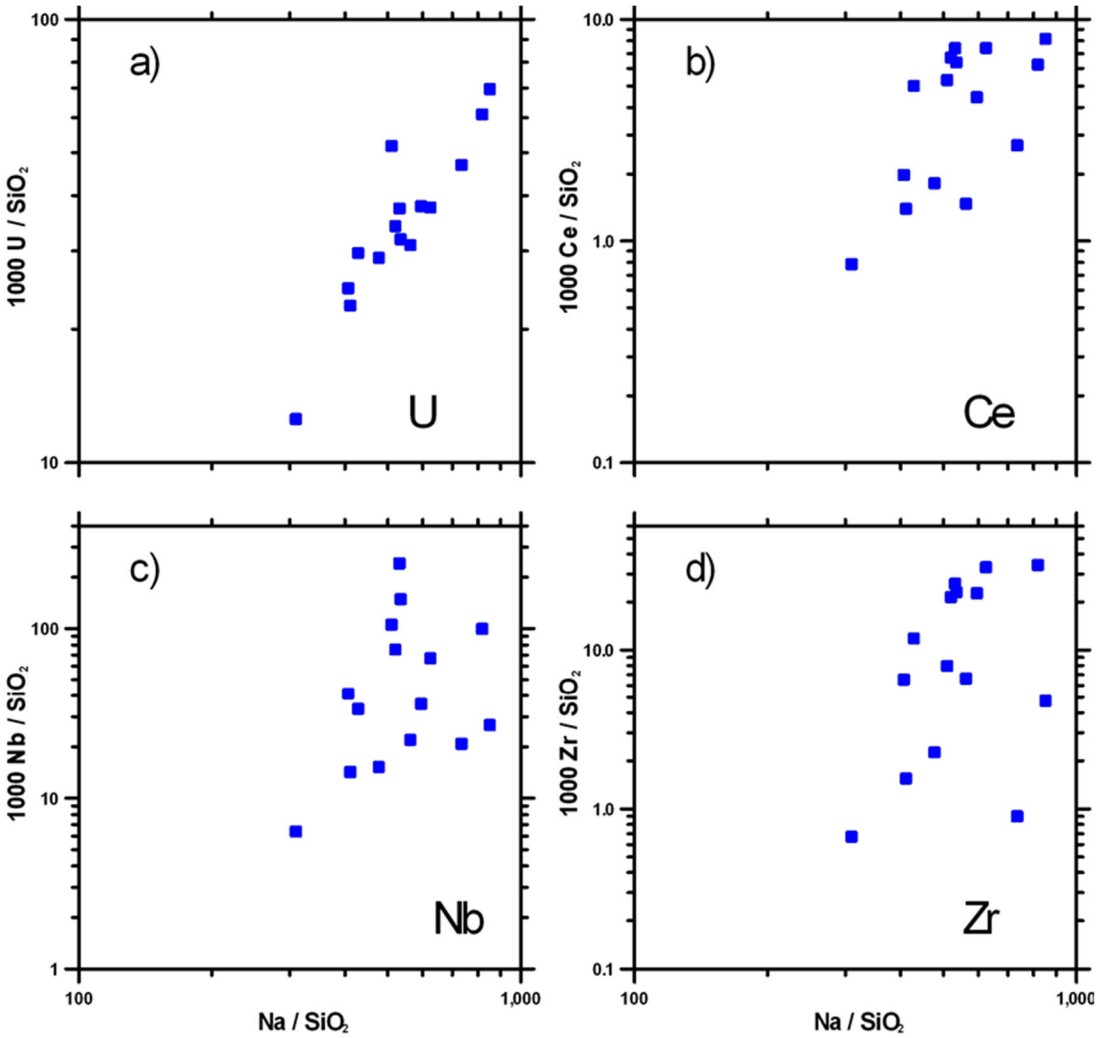

Figure 33: Slag source for trace elements: Cross-plots of Na / SiO_2 with a) U / SiO_2; b) Ce / SiO_2; c) Nb / SiO_2; (d) Zr / SiO_2.

Sorption control on trace elements concentrations in leachate

Sorption of trace elements on colloidal iron or manganese oxyhydroxides can exert significant control on their aqueous mobility. Geochemical cross-plots of filtered (< 0.45 µm) or "dissolved" versus unfiltered or "total" concentrations are used here to assess sorption control for selected trace and rare earth elements.

Plots of particulate (unfiltered minus filtered) concentrations of Mn and Ce versus particulate Fe (Figure 34) exhibit strong correlations, which suggests that Fe colloids are the main sorbent in slag leachate. The source of Fe is unclear although it may be columbite or taenite (Table 5).

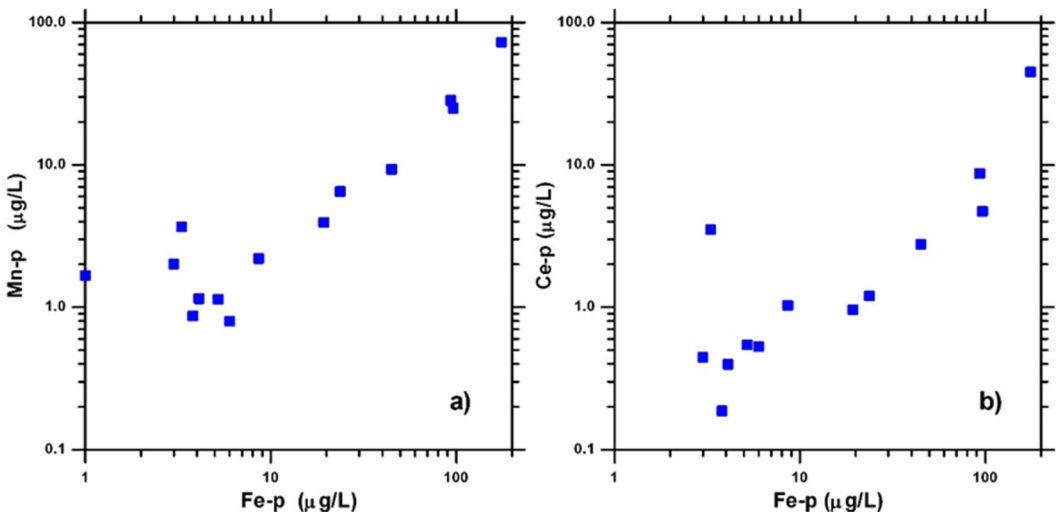

Figure 34: Sorption **c**ontrol on trace element concentrations: Cross-plots of particulate (colloidal) trace metal concentration versus particulate Fe concentrations: a) Mn; b) Ce.

For REEs, cross-plots of filtered versus unfiltered concentrations (Figure 35) indicate a range of sorption control. Cerium concentrations are dominated by the colloidal fraction whereas concentrations of Eu, Dy and Yb are dominated by the dissolved fraction. The degree of sorption control on REEs in leachate appears to decrease with atomic number. This observation is explored further in Figure 36, which shows REE profiles for both filtered and unfiltered samples. A comparison of these profiles confirms that the colloidal (> 0.45 µm) fraction of REE concentrations decreases from La to Lu. An interesting feature of this figure is the strong positive Eu anomaly in the REE profiles indicating preferential dissolution of a Eu(II)-bearing host.

Filtered and total concentrations of Al, U, Nb and Zr are essentially identical (Figure 37). All of these elements appear to be in the form of aqueous species in the slag leachate. Their concentrations range from elevated to very high and are not limited by sorption processes under conditions of the leach experiment.

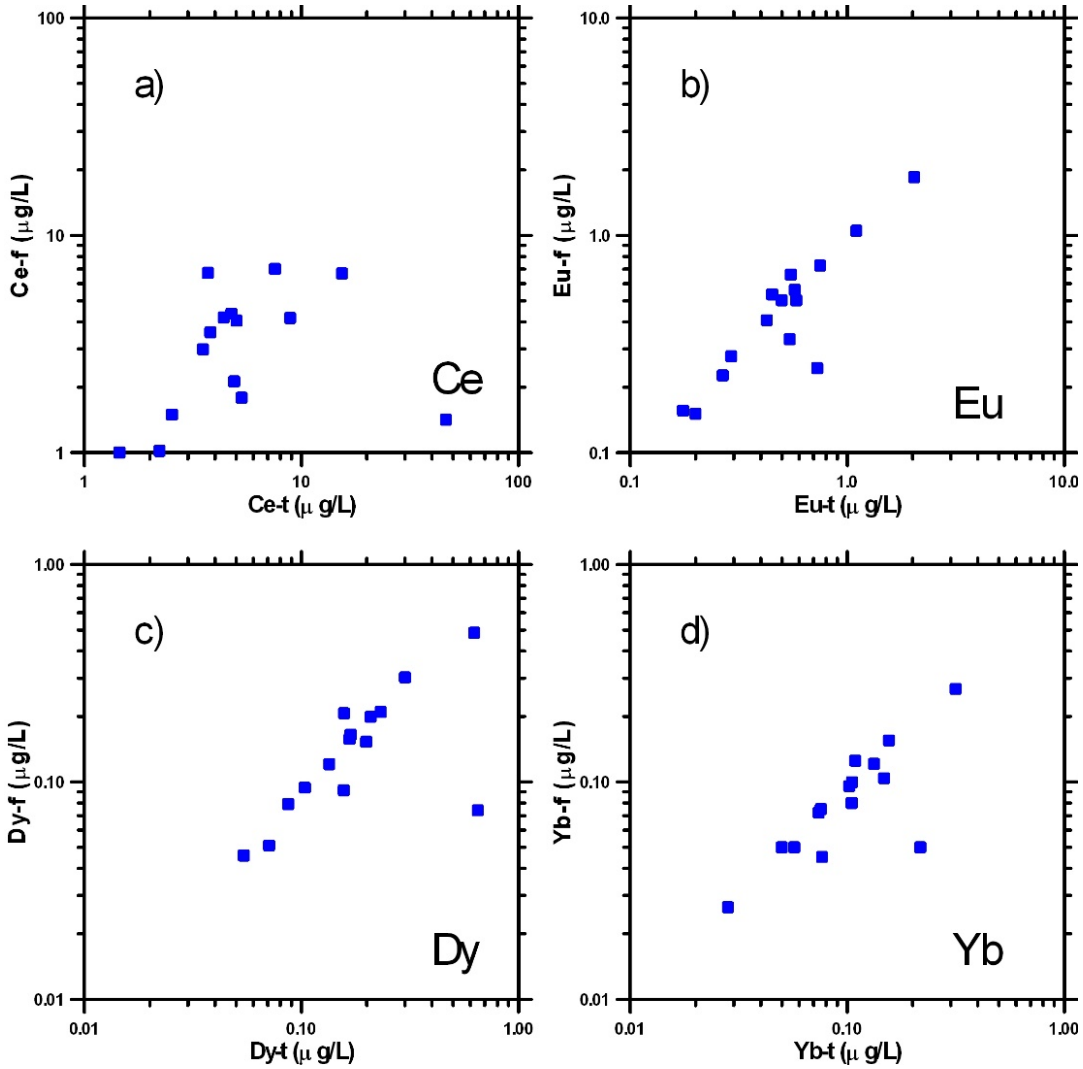

Figure 35: Sorption control on rare earth element concentrations: Cross-plots of filtered versus unfiltered (total) concentrations of a) Ce; b) Eu; c) Dy; d) Yb.

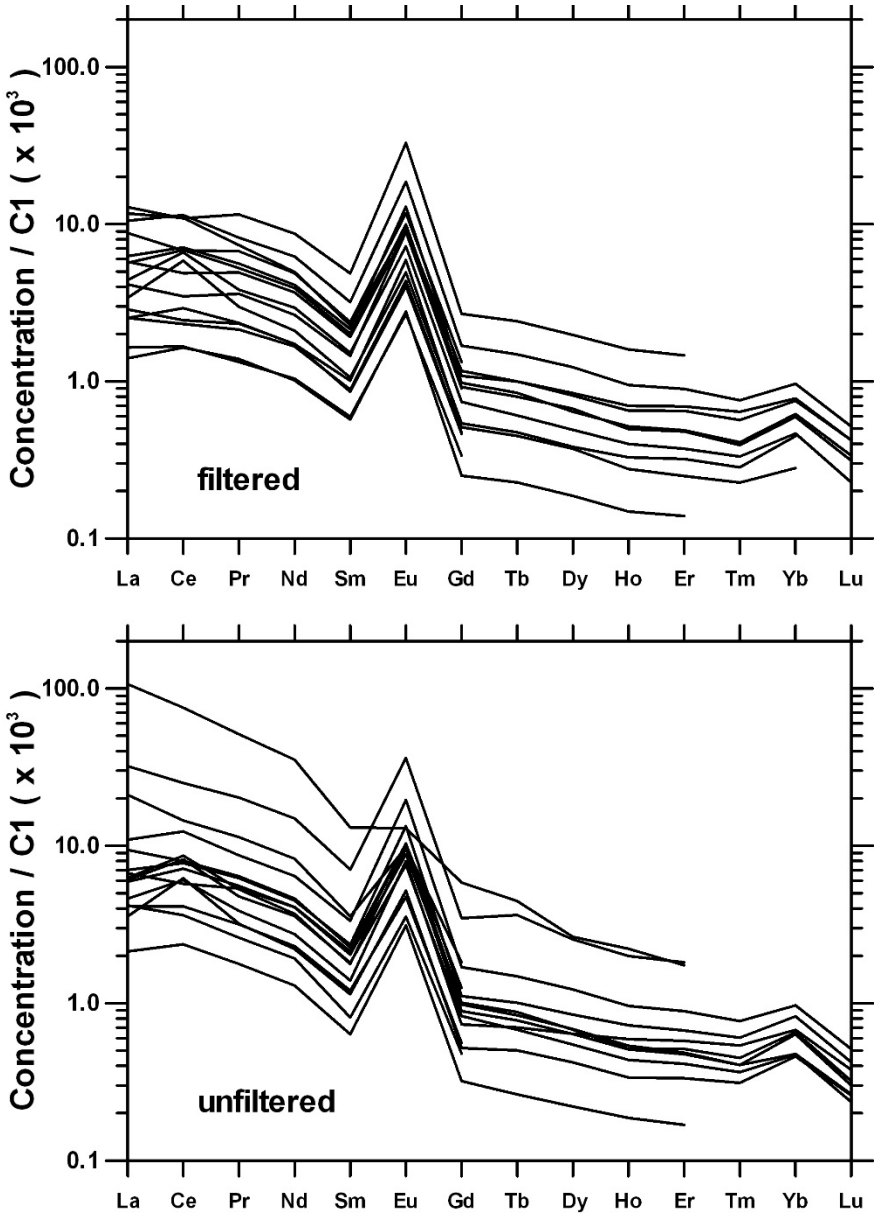

Figure 36: Chondrite-normalized REE patterns for slag leachate: (top) filtered or dissolved concentrations; (bottom) unfiltered or total concentrations. C1-chondrite abundances are from McDonough and Sun (1995).

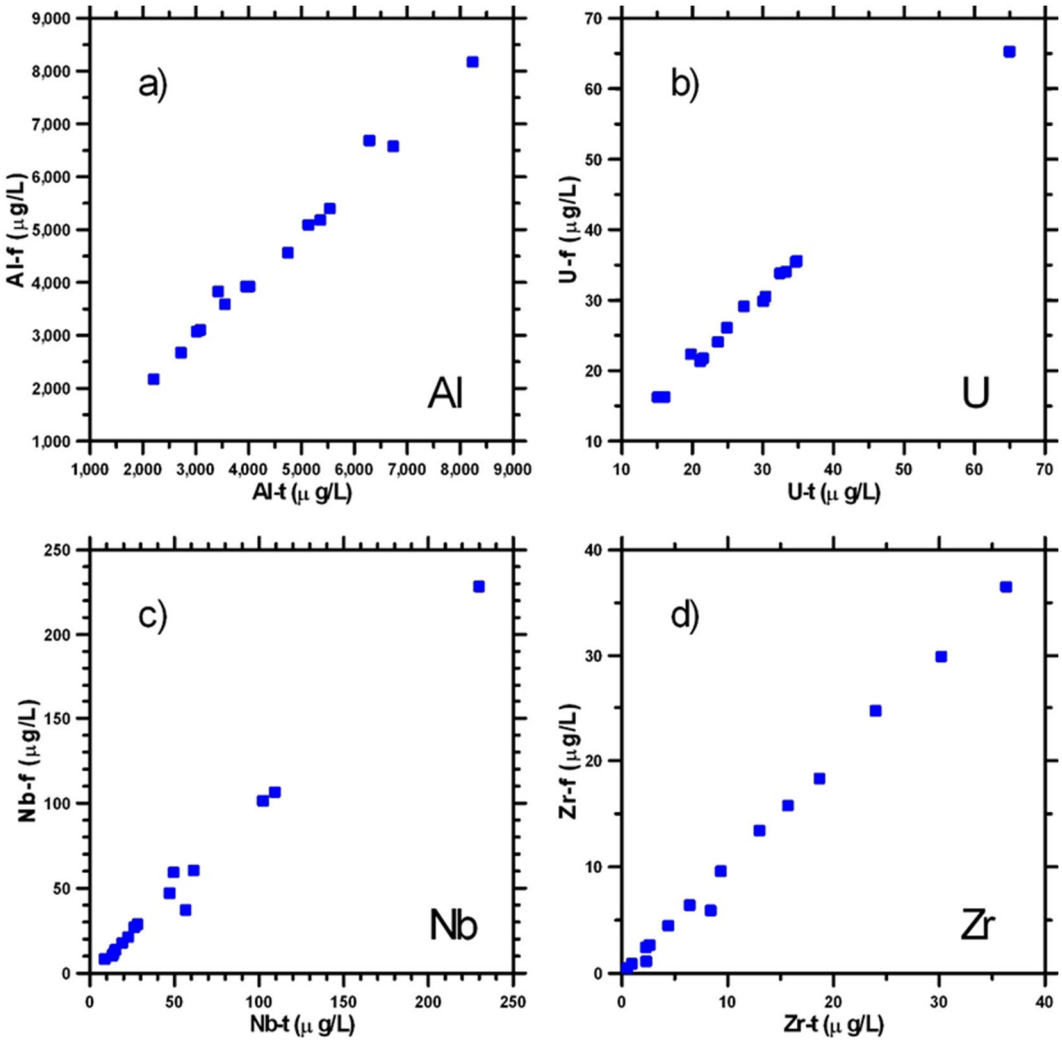

Figure 37: Sorption **c**ontrol on trace element concentrations: Cross-plots of filtered versus unfiltered (total) concentrations of a) Al; b) U; c) Nb; d) Zr.

5.2 Comparisons with results of previous studies

Slag from the aluminothermic conversion of pyrochlore concentrates contains radioactivity at levels significantly higher than the natural background. Release of radioactivity and other potential contaminants from the slag depends on its weathering and leaching properties. These properties are a function of its physical, chemical, and mineralogical composition (Veblen et al., 2004). The slag contains both crystalline and glass phases, and its weathering is controlled by those phases most susceptible to attack from the elements. These factors, together with local climatic conditions including temperature, precipitation intensity and chemistry, determine the rate at which uranium and other species are leached (Veblen et al., 2004).

Mitchell and Mariano (2016) investigated primary phases in ferroniobium slags from carbonatite-hosted deposits at Araxá (Brazil), Oka (Québec) and Fen-Søve (Norway). While the phases present were a function of the composition of the local pyrochlore feed and the particular reagents used in the conversion process, the slags shared key characteristics: All slags were enriched in U and Th and none contained any Fe-bearing compounds. They were modally-dominated by crystalline beta-alumina or hibonite and a wide variety of Th-Ba-Ti-Nb-Al-oxide compounds, with silico-aluminate glasses in interstices between crystals. At Fen-Søve, the phases identified, in order of crystallization, were beta-alumina and Ba-Ti-niobate, Zr-Ti-Th-niobate, Nb-Th bearing zirconolite, diverse Th-Nb-rich and Al-poor perovskites, and a Na-rich silicate glass. An earlier study of Fen-Søve slag (RBTV, 2005) identified the main Al-oxide phases as Ti-Ba-Mg-diaoyudaoite, hibonite, and Mg-Al-spinel. Mitchell and Mariano (2016) found that slag from Oka consisted of a framework of hibonite with interstitial Ca-zirconate and Al-REE rich perovskites set in F-Na-Ce calcium aluminate glass. Uranium was found in the Ca-zirconate, perovskite and glass. The phases identified in this study (Table 5) are in general agreement although uraninite was found to be a U host, and columbite and taenite were minor Fe hosts. Veblen et al. (2004) investigated slags produced from the aluminothermic conversion of Nb-rich smelter slags rather than from pyrochlore concentrates. Generally, they contain more SiO_2 and less Al_2O_3 than the Oka slags. Nonetheless, the main phases are similar. Slag from their site B, which appears to most resemble the Oka slag physically, consists of (in order of decreasing modal abundance) gehlenite, glass, clinopyroxene, perovskite, calzirtite, zirconolite, and rutile. The main U-bearing phases were found to be glass, perovskite, calzirtite, and zirconolite. In Oka slag, Balkwill-Tweedie (2020) identified hibonite, perovskite, grossite, calcium zirconate, and beta-alumina in variable proportions depending on slag zonation. F-Na-Ce calcium aluminosilicate glass was found in decreasing proportion from top to bottom. Fluorite was found in the top zone whereas gehlenite, hercynite and columbite were found in the bottom zone

The slags investigated by Veblen et al. (2004) were 40 years old or less yet they all exhibited demonstrable signs of weathering. The weathering formed a rind on external slag surfaces and propagated inwards along grain boundaries and fractures. The authors found that weathering of slag was incongruent, with preferential dissolution of certain phases. Glass and perovskite were found to be the most unstable phases under oxidizing, near-surface conditions. Glass being the last phase to form, filled interstices among earlier-formed crystalline phases. Therefore, glass dissolution and devitrification, both which increase slag porosity, makes these minerals more

accessible to alteration and leaching by infiltrating waters. The authors observed clear evidence of metal leaching from mineral grains adjacent to voids and fractures. Because U and Th were hosted by phases of different weathering susceptibility, the authors concluded that their bulk leaching rate will vary over time as difference source phases are depleted within the slag. Weathering of Oka slag has yet to be investigated at the same level of detail; however, some similar observations can be made. With an average age of about 45 years, Oka slag exhibits a range of weathering, from minimal (Figure A-3) to complete disintegration (Figure A-8). The degree of weathering appears to depend on slag zonation, with less weathering in the massive-textured tops of the melt buttons and more in their lower vesicular portion (Figure A-4). At Canadian latitudes, freeze-thaw action is an important physical weathering mechanism that enhances chemical processes discussed by Veblen et al. (2004).

Leaching of heavy metals, U, Th, and their radionuclide daughter products from ferroniobium slag represents a potential threat to surface and groundwater quality. As part of the environmental assessment for the proposed Niocan niobium mine project, standard leach tests were performed on samples of slag from the nearby SLC site. Results from these tests are compared with results of the field-scale leach experiment conducted in this study (Table 10). With respect to Al and F, there is qualitative agreement between this study and the previous work in that leachate concentrations are elevated. With respect to U, concentrations observed in this study are significantly higher than those observed in the laboratory tests. Analyses of radionuclides in slag leachate were not performed as part of this study. However, radionuclide analyses in leachate from SLC and Niobec slags are presented in supporting documentation for the Niocan project environmental assessment and are reproduced here for ease of reference (Table 11).

Radioactivity measurements on ferroniobium slag solids have been reported previously from the SLC mine, the Niobec mine, and the former Søve-Fen mine. All three mines are hosted by carbonatite intrusions. Concentrations of radioelements in ferroniobium slag from three unidentified processing facilities were reported by Veblen et al. (2004). A summary compilation of radioelement and activity concentrations from this study and from these past reports is presented in Table 12. Allowing for the variable number of samples in each study, measurements of slag radioactivity at the Oka mine site are fairly consistent. Slag radioactivity levels at the Niobec and Søve-Fen mines appear higher although this may be an artefact of conservative sample selection. Slag radioactivity measurements from the processing plants span wider ranges reflecting more diverse feedstocks and waste forms.

The International Atomic Energy Agency (Wymer, 2006) has identified the production of niobium and ferroniobium as an industrial activity likely to require regulatory assessment for radiation protection of workers. The radioactivity results for slag at the former SLC mine support this conclusion and the need for long-term management of the technologically enhanced NORM on the site (Health Canada, 2014).

Table 10: Chemical analyses of leachate from Oka slags. Results for EPA-1311 and EPA-1312 tests are from Table 12.1 of BAPE (2003). Results for this study are averages of 15 analyses (filtered samples) from barrels 2, 3, and 4 (prior to the addition of mine tailings). Note difference in units between this study and the previous work. Below detection (<). Not analyzed (-).

	EPA-1311		EPA-1312		This Study
	04/2002 (mg/L)	09/2002 (mg/L)	04/2002 (mg/L)	09/2002 (mg/L)	Leachate (µg/L)
Ag	-	0.013	-	0.005	0.05
Al	-	70	-	190	4532
As	< 0.01	< 0.01	< 0.01	< 0.01	1.14
B	< 1	< 1	< 1	< 1	9.85
Ba	5.4	4.4	3.3	2.5	24.83
Cd	< 0.005	< 0.005	< 0.005	< 0.005	0.10
Cr	< 0.02	< 0.01	< 0.02	< 0.01	3.32
Cu	-	0.01	-	< 0.01	7.41
F	15	14	5.3	5.9	27407
Mn	-	0.37	< 0.01	< 0.01	3.35
Mo	-	< 0.05	-	< 0.05	4.43
Ni	-	0.02	-	< 0.02	0.99
Pb	< 0.05	< 0.003	< 0.01	< 0.003	0.24
Sb	-	< 0.01	-	< 0.01	0.41
Se	< 0.01	< 0.01	-	< 0.01	4.66
U	< 0.005	< 0.005	-	< 0.005	29.45
Zn	-	0.39	-	0.02	4.19

Table 11: Radiological analyses of ferroniobium slag leachate from the SLC mine at Oka (BAPE-DA21, 2002) and the Niobec mine (BAPE-DB46.1, 2002). Below detection (<).

Radionuclide	SLC (Oka) Sample 104119E Activity		Niobec Sample P020419 Activity		Niobec Sample S-3 Activity	
	Measured Bq/L	Estimated Bq/L	Measured Bq/L	Estimated Bq/L	Measured Bq/L	Estimated Bq/L
Th-232 Series						
Th-232						
Ra-228						1300
Ac-228	< 2		< 2		1300	
Th-228						
Ra-224						20
Rn-220						20
Po-216						20
Pb-212	< 1		< 1		19.9	
Bi-212	< 7		< 7		20	
Po-212						14.9
Tl-208	< 1		< 1		5.1	
U-238 Series						
U-238						
Th-234						
Pa-234	< 100		< 100		< 100	
U-234						
Th-230						
Ra-226	17		5		246	
Rn-222		18				105
Po-218		18				105
Pb-214	20		< 0.5		108	
Bi-214	20		< 0.5		102	
Po-214		18				105
Pb-210		18				
Bi-210		18				
Po-210		18				
U-235	0.7		< 0.5		< 0.5	
K-40	< 6		8		92	
Total	57.7	108	13	0	1893	1689.9

Table 12: Radioactivity of ferroniobium slag from different sources. If the number of samples (n) is greater than 1, the range of observations is given. Below detection (<). Not analyzed (-).

	n	U (ppm)	Th (ppm)	U-238 (Bq/g)	Ra-226 (Bq/g)	Th-232 (Bq/g)	Ac-228 (Bq/g)
Oka[1]	3	386-2227	1265-2492	4.80-27.5	4.00-26.0	5.1-10.1	5.2-10.0
Oka[2]	37	455-1616	607-5069	-	-	-	-
Oka[3]	20	-	-	0.04-21.0	0.08-40.0	0.03-9.4	-
Oka[4]	3	814	1829	10.06-23.1	10.06-13.47	7.33-48.5	7.66-62.38
Niobec[5]	2	1900-2800	8300-8700	-	22-32	-	32-33
Søve-Fen[6]	1	3588	11750	-	46.0	47.0	-
NUREG[7]	14	9-1980	23-13250	-	-	-	-

[1] this study; chemical analyses; see Table 7
[2] this study; spectral gamma radiometric analyses; see Table 9
[3] WSP (2018), Table 23
[4] BAPE-DA21, Annex II, tables 3,4; Annex III, Table 7
[5] BAPE-DB46, Annex 4
[6] RTBV (2005), p.12
[7] Veblen et al. (2004), table 2.5

6.0 SUMMARY AND CONCLUSIONS

Between 1961 and 1976, the St. Lawrence Columbium mine produced pyrochlore concentrate from a niobium-bearing carbonatite deposit near Oka, Québec. Beginning in 1971, the pyrochlore concentrate was converted into ferroniobium alloy through an aluminothermic reduction process, which also yielded slag as a waste product. Uranium and thorium occurring as impurities within the pyrochlore are preferentially sequestered in the slag. This report is concerned with the environmental characteristics of the slag including its physical properties, mineralogy, chemistry, radioactivity, and the chemistry of its leachate.

Slag buttons were deposited on the mine site at the ground surface and exposed to the elements. After approximately 45 years of weathering, the upper, massive, portion of the buttons appears relatively intact, whereas the lower, vesicular, portion of the slag crumbles readily.

Geochemically, the slag is composed mainly of aluminum, calcium and sodium from reagents, impurities from the pyrochlore concentrate, including titanium, silicon, zirconium, uranium, thorium, and rare earth elements, as well as unrecovered niobium. The slag forms an assemblage of high-temperature phases consisting of hibonite, beta-alumina, calcium zirconate, perovskite and glass. The minerals deviate significantly from their ideal compositions as they incorporate rare earth and other trace elements including uranium and thorium.

Radiological analyses for U-238, U-235, Th-232 and their daughter products were performed on three selected slag samples. Results indicated approximate secular equilibrium within the decay chains. Activity concentration ranges for the U-238, U-235 and Th-232 series were 67-385 Bq/g, 2-14 Bq/g and 56-111 Bq/g, respectively. The highest total activity concentration was 456 Bq/g.

A ground-based spectral radiometric survey was conducted on a longitudinal transect through the slag disposal area. Uranium equivalent concentrations ranged between 455 and 1616 ppm, with a median value of 1069 ppm. Thorium equivalent concentrations ranged between 607 and 5059 ppm, with a median value of 2101 ppm. Assuming secular equilibrium of the decay series, total activity concentrations of the slag varied between 126 and 417 Bq/g, with a median of 304 Bq/g.

An on-site field-scale leach test was conducted using three 220 L barrels of coarse vesicular slag open to natural precipitation. The experiment ran from June of 2017 to November of 2018 during which time collected leachate was sampled six times. The cumulative flux through the barrels was 85 L, which is equivalent to approximately 2 pore volumes. The leachate had a pH of 9.2, which was steady throughout the duration of the test. Total dissolved solids varied erratically with specific conductances ranging between 1191 and 3280 µS/cm. Leachate chemistry did not stabilize during the test likely because seasonal freeze-thaw cracking of the slag was regularly exposing fresh surfaces to chemical weathering. The main solutes were sodium and bicarbonate. Fluoride concentrations varied between 16.8 and 45.6 mg/L. Dissolved aluminum and uranium concentrations reached as high as 8173 and 65 µg/L, respectively. Uranium appears to leach readily from glass phases in the slag. Results of the study show that ferroniobium slag is a technologically-enhanced naturally occurring radioactive material (TENORM) requiring long-term environmental management.

REFERENCES

Aitchison, J., 1986. The statistical analysis of compositional data; Chapman and Hall, London, 416 p.

Balkwill-Tweedie, H., 2020. Effects of weathering on leaching properties of slag from a niobium mine, Oka, Québec; M.Sc. thesis, University of Ottawa, Ottawa, Ontario, 66 p.

BAPE, 2002. Projet d'exploitation d'une mine et d'une usine de niobium à Oka; Rapport d'enquête 167, Bureau d'Audiences Publiques sur l'Environnement, Québec, 106 p. https://www.bape.gouv.qc.ca/fr/dossiers/exploitation-une-mine-une-usine-niobium-oka/

BAPE-DA21, 2002. Caractérisation des matériaux du site minier St-Lawrence Columbium; Roche Ltée, mai 2002. https://www.bape.gouv.qc.ca/fr/dossiers/exploitation-une-mine-une-usine-niobium-oka/documentation/

BAPE-DB46, 2002. Rapport d'actualisation des activités de la mine Niobec; Ministère de l'Environnement du Québec, Direction régionale du Saguenay – Lac-Saint-Jean, mars 2002. https://www.bape.gouv.qc.ca/fr/dossiers/exploitation-une-mine-une-usine-niobium-oka/documentation/

BAPE-DB46.1, 2002. Résultats des analyses d'échantillons de scorie, du lixiviat des scories, du ferroniobium (FeNb), du lixiviat des résidus miniers, des analyses radiologiques sur le solide – parc à résidus Niobec, Mine Niobec; https://www.bape.gouv.qc.ca/fr/dossiers/exploitation-une-mine-une-usine-niobium-oka/documentation/

BAPE, 2003. Les effets potentiels du projet d'exploitation d'une mine et d'une usine de niobium à Oka sur les eaux de surface et les eaux souterraines ainsi que leurs utilisations; Project minier Niocan, Étude environnementale, Rapport complémentaire II, Roche Ltée, janvier 2003. https://www.bape.gouv.qc.ca/fr/dossiers/effets-potentiels-exploit-une-mine-une-usine-niobium-oka-eaux-surface-souterraines-utilisations/

BAPE, 2005. Les effets potentiels du projet d'exploitation d'une mine et d'une usine de niobium à Oka sur les eaux de surface et les eaux souterraines ainsi que leurs utilisations; Rapport d'enquête 208, Bureau d'Audiences Publiques sur l'Environnement, Québec, 93 p. https://www.bape.gouv.qc.ca/fr/dossiers/effets-potentiels-exploit-une-mine-une-usine-niobium-oka-eaux-surface-souterraines-utilisations/

Berger, V. I., Singer, D.A., and Orris, G.J., 2009. Carbonatites of the world, explored deposits of Nb and REE - Database and grade and tonnage models; U. S. Geological Survey Open-File Report 2009-1139, 17 p. and database.

Carbonneau, C., and Caron, J.C., 1965. The production of pyrochlore concentrates at St. Lawrence Columbium and Metals Corp.; Trans. Can. Inst. Min., v. 68, p. 71-79.

Chen, W., and Simonetti, A., 2013. In-situ determination of major and trace elements in calcite and apatite, and U-Pb ages of apatite from the Oka carbonatite complex: Insights into a complex crystallization history; Chemical Geology, v. 353, p. 151-172. doi:10.1016/j.chemgeo.2012.04.022

Desbarats, A.J., Percival, J.B., Pelchat, P., Sekerka, J., Bilot, I., Girard, I., and Gammon, P., 2020. Geoenvironmental characterization of carbonatite tailings, Saint Lawrence Columbium mine, Oka, Québec; Geological Survey of Canada Open File 8753, 98 p.

Des Roches, S., 2020. Environmental characterization of waste rock and tailings from a carbonatite-hosted niobium and rare earth element deposit; M.Sc. thesis, Queen's University, Kingston, Ontario, 239 p.

ECCC, 2018. Canadian Climate Normals, Environmental and Climate Change Canada; website accessed in May, 2018. http://climate.weather.gc.ca/climate_normals

Ecozones, 2014. The Ecological Framework of Canada; Website accessed in 2018. http://ecozones.ca

Edahbi, M., Plante, B., Benzaazoua, M., Kormos, L., and Pelletier, M., 2018a. Rare earth elements (La, Ce, Pr, Nd, and Sm) from a carbonatite deposit: Mineralogical characterization and geochemical behavior; Minerals, v.8, no. 55. doi:10.3390/min8020055

Edahbi, M., Plante, B., Benzaazoua, M., and Pelletier, M., 2018b. Geochemistry of rare earth elements within waste rocks from the Montviel carbonatite deposit, Québec, Canada; Environmental Science and Pollution Research., v. 25, no. 11, p. 10997-11010. doi.org/10.1007/s11356-018-1309-7

Ford, K. L., Savard, M., Dessau, J.-C., Pellerin, E., Charbonneau, B.W., and Shives, R.B.K., 2001. The role of gamma-ray spectrometry in radon risk evaluation: A case history from Oka, Québec; Geoscience Canada, v. 28, no. 2, p. 59-64.

Geological Survey of Canada, 1996. Airborne Geophysical Survey, Oka, Québec; NTS / SNRC 31 G/8, G/9, H/5, H/12. Geological Survey of Canada, Open File 3417, scale 1:50 000.

Gold, D. P., Vallée, M., and Charette, J.P., 1967. Economic geology and geophysics of the Oka Alkaline Complex, Quebec; Canadian Institute of Mining and Metallurgy Bulletin, v. 60, p. 1131-1144.

Gold, D. P., and Vallée, M., 1969. Field Guide to the Oka Area: Description and Itinerary; Government of Québec, Department of Natural Resources, Mines Branch, Rep. S-101, 37p.

Gupta, C.K., and Suri, A.K., 1994. Extractive metallurgy of niobium. CRC Press, Boca Raton, FL, 272 p.

Health Canada, 2014. Canadian Guidelines for the Management of Naturally Occurring Radioactive Materials (NORM); Prepared by the Canadian NORM Working Group of the Federal Provincial Territorial Radiation Protection Committee – Revised 2011, April 2014.

Huang, X., Zhang, G., Pan, A., Chen, F., and Zheng, C., 2016. Protecting the environment and public health from rare earth mining; Earth's Future, v. 4. doi:10.1002/2016EF000424.

Lentz, D., Eby, N., Lavoie, S., and Park, A., 2006. Diatremes, dykes, and diapirs: Revisiting the ultra-alkaline to carbonatitic magmatism of the Monteregian Hills; Guide book, Field Trip B4, GAC/MAC Joint Annual Meeting, Montréal, Québec, 48 p.

Lumpkin, G. R., Gao, Y., Gieré, R., Williams, C.T., Mariano, A.N., and Geisler, T., 2014. The role of Th-U minerals in assessing the performance of nuclear waste forms; Mineralogical Magazine, v. 78, no. 5, p. 1071-1095. doi:10.1180/minmag.2014.078.5.01

McDonough, W. F., and Sun, S., 1995. The composition of the Earth; Chemical Geology, v. 120, p. 223-253.

Mitchell, R. H., 2015. Primary and secondary niobium deposits associated with carbonatites; Ore Geology Reviews, v. 64, p. 626-641. doi.org/10.1016/j.oregeorev.2014.03.010.

Mitchell, R. H., and Mariano, A.N., 2016. Primary phases in aluminous slags produced by the aluminothermic reduction of pyrochlore; Mineralogical Magazine, v. 80, no. 2, p. 383-397. doi:10.1180/minmag.2016.080.009.

Modreski, P. J., T.J. Armbrustmacher, and D.B. Hoover, 1995. Carbonatite deposits; In chapter 6 of Preliminary Compilation of Descriptive Geoenvironmental Mineral Deposit Models, (ed.) E.A. du Bray, U.S. Geological Survey, Open-File Report 95-831, p. 47-49.

Nastev, M., Rivera, A., Lefebvre, R., Martel, R., and Savard, M., 2005. Numerical simulation of groundwater flow in regional rock aquifers, southwestern Quebec, Canada; Hydrogeology Journal, v. 13, p. 835-848. doi:10.1007/s10040-005-0445-6.

Nesbitt, H. W., Bancroft, G.M., Fyfe, W.S., Karkhanis, S.N., Nishijima, A., and Shin, S., 1981. Thermodynamic stability and kinetics of perovskite dissolution; Nature, v. 289, p. 358-362.

NIOCAN, 2010. Modèle géologique et estimation des ressources de niobium de la zone S-60, Oka, Québec; NI 43-101 Technical Report, prepared by S. Lavoie and J.-C. Caron for Niocan Inc., 182 p.

Paschoa, A.S., 1998. Potential environmental and regulatory implications of naturally occurring radioactive materials; Applied Radiation and Isotopes, v. 49, no. 3, p. 189-196.

Petruk, W., and Owens, D.R., 1975. Electron microprobe analyses for pyrochlores from Oka, Quebec; Canadian Mineralogist, v. 13, p. 282-285.

RBTV, 2005. Miljøgeologisk undersøkelse av lavradioaktivt slagg fra ferroniobproduksjonen ved Norsk Berverk PÅ Søve 1956-1965; Regiongeologen For Buskerud, Telemark, Vestfold, Rapport nr. 1, 2005, pp.48. (in Norwegian)

Richardson, D. G., and Birkett, T.C., 1996. Carbonatite-associated deposits; In: Geology of Canadian Mineral Deposit Types, (eds.) O.R. Eckstrand, W.D. Sinclair, and R.I. Thorpe, Geology of Canada Series, No. 8, p. 541-558, Geological Survey of Canada, Ottawa, Ontario.

RRSSSL, 1998. Le radon à Oka – Rapport d'intervention de santé publique; Régie Régionale de la Santé et des Services Sociaux des Laurentides, report, 134 p., http://www.bape.gouv.qc.ca/sections/archives/oka/docdeposes/documdeposes/DB17.pdf

RRSSSL, 1999. L'uranium dans l'eau des puits domestiques à Oka, 1999; Régie Régionale de la Santé et des Services Sociaux des Laurentides, report, 26p. and annexes, http://www.bape.gouv.qc.ca/sections/archives/oka/docdeposes/documdeposes/DB18.pdf

Schultz, K.J., Piatak N.M., and Papp, J.F., 2017. Niobium and Tantalum; chapter M in Critical mineral resources of the United State – Economic and environmental geology and prospects for future supply, (eds.) K.J. Schultz, J.H. DeYoung Jr., R.R. Seal II, and D.C. Bradley, U.S. Geological Survey, Professional Paper 1802–M, Reston, VA. p. M1– M34. doi.org/10.3133/pp1802M.

Simandl, G. J., Paradis, S., 2018. Carbonatites: related ore deposits, resources, footprint, and exploration methods; Applied Earth Science. doi.org/10.1080/25726838.2018.1516935

SLC, 1962. St. Lawrence Columbium and Metals Corporation, Annual Report, 8 p.

SLC, 1963. St. Lawrence Columbium and Metals Corporation, Annual Report, 8 p.

SLC, 1964. St. Lawrence Columbium and Metals Corporation, Annual Report, 16 p.

SLC, 1966. St. Lawrence Columbium and Metals Corporation, Annual Report, 28 p.

SLC, 1967. St. Lawrence Columbium and Metals Corporation, Annual Report, 16 p.

SLC, 1968. St. Lawrence Columbium and Metals Corporation, Annual Report, 18 p.

SLC, 1969. St. Lawrence Columbium and Metals Corporation, Annual Report, 24 p.

SLC, 1970. St. Lawrence Columbium and Metals Corporation, Annual Report, 24 p.

SLC, 1971. St. Lawrence Columbium and Metals Corporation, Annual Report, 20 p.

SLC, 1972. St. Lawrence Columbium and Metals Corporation, Annual Report, 28 p.

Steger, H.F., and Bowman, W.S., 1981. Niobium Ore Oka-1 – A Certified Reference Material; Canada Centre for Mineral and Energy Technology (CANMET) report 81-1E, Energy, Mines and Resources Canada, Ottawa, 16 p.

Strong, W.L., Zoltai, S.C., and Ironside, G.R., 1989. Ecoclimatic regions of Canada; Ecological Land Classification Series 23, Can. Wildlife Service, Environment Canada, Ottawa, 122 p.

USEPA, 2012. Rare Earth Elements: A Review of Production, Processing, Recycling, and Associated Environmental Issues; United States Environmental Protection Agency Report EPA/600/R-12/572, Cincinnati, OH, 135 p.

Vallières, M., 1989. Des mines et des hommes – Histoire de l'industrie minérale québécoise des origines au début des années 1980; Les Publications du Québec, Gouvernement du Québec, 439 p.

Veblen, L. A., Farthing, D., O'Donnell, E., and Randall, J.D., 2004. Characterization of radioactive slags; Office of Nuclear Regulatory Research, U.S. Nuclear Regulatory Commission, Washington, D.C, NUREG-1703, 92 p.

Verplanck, P. L., and Van Gosen, B.S., 2011. Carbonatite and alkaline intrusion-related rare earth element deposits - A deposit model; U.S. Geological Survey Open File 2011-1256, 6 p.

Verplanck, P. L., Van Gosen, B.S., Seal, R.R. II, and McCafferty, A.E., 2014. A deposit model for carbonatite and peralkaline intrusion-related rare earth element deposits; U.S. Geological Survey Science Investigations Report 2010-5070-J, 58 p. doi.org/10.3133/sir20105070J.

Weng, Z. H., Jowitt, S.M., Mudd, G.M., and Haque, N., 2013. Assessing rare earth element mineral deposit types and links to environmental impacts; Applied Earth Science (Trans. Austral. Inst. Min. Metall. B), v. 122, no. 2, p. 83-96. doi:10.1179/1743275813Y.0000000036.

WSP, 2018. Caractérisation environnementale, Site minier St-Lawrence Columbium, Oka (Québec); report prepared for le Ministère de l'Énergie et des Ressources Naturelles by WSP Canada Inc., March 2018, 61p. and appendices. https://mern.gouv.qc.ca › demande-acces › document_19-04-003-C

Wymer, D. G., 2006. Assessing the need for radiation protection measures in work involving minerals and raw materials; International Atomic Energy Agency Safety Reports Series 49. International Atomic Energy Agency, Vienna, 66 p.

Zurevinski, S. E., and Mitchell, R.H., 2004. Extreme compositional variation of pyrochlore-group minerals at the Oka carbonatite complex, Quebec: Evidence of magma mixing? Canadian Mineralogist, v. 42, p. 1159-1168.

APPENDIX

PHOTOGRAPHS OF FERRONIOBIUM SLAG

Figure A-1: Top view of a partial slag button exhibiting a ropy texture on its surface. Photograph by A.J. Desbarats. NRCan Photo Database number 2020-621.

Figure A-2: Top view of a slag button exhibiting a massive texture with a smooth surface and a polygonal crack pattern. Photograph by A.J. Desbarats. NRCan Photo Database number 2020-622.

Figure A-3: Cross-section of a slag button exhibiting a massive texture with horizontal vugs. Photograph by A.J. Desbarats. NRCan Photo Database number 2020-623.

Figure A-4: Cross-section of a slag button exhibiting a sharp transition from a massive texture with polygonal cracks to a highly altered vesicular texture. Photograph by A.J. Desbarats. NRCan Photo Database number 2020-624.

Figure A-5: Cross-section of a slag button exhibiting a transition from a weathered massive texture with polygonal cracks to a highly altered vesicular texture. Photograph by A.J. Desbarats. NRCan Photo Database number 2020-625.

Figure A-6: Top view of a slag button exhibiting a weathered massive texture with polygonal cracks and an underlying layer of slag with a spongy texture. Photograph by A.J. Desbarats. NRCan Photo Database number 2020-626.

Figure A-7: Top view of a slag button exhibiting a weathered massive texture on its surface with polygonal cracks and underlying highly weathered material with a vesicular texture. Photograph by A.J. Desbarats. NRCan Photo Database number 2020-627.

Figure A-8: Extremely weathered slag with a vesicular texture. Photograph by A.J. Desbarats. NRCan Photo Database number 2020-628.

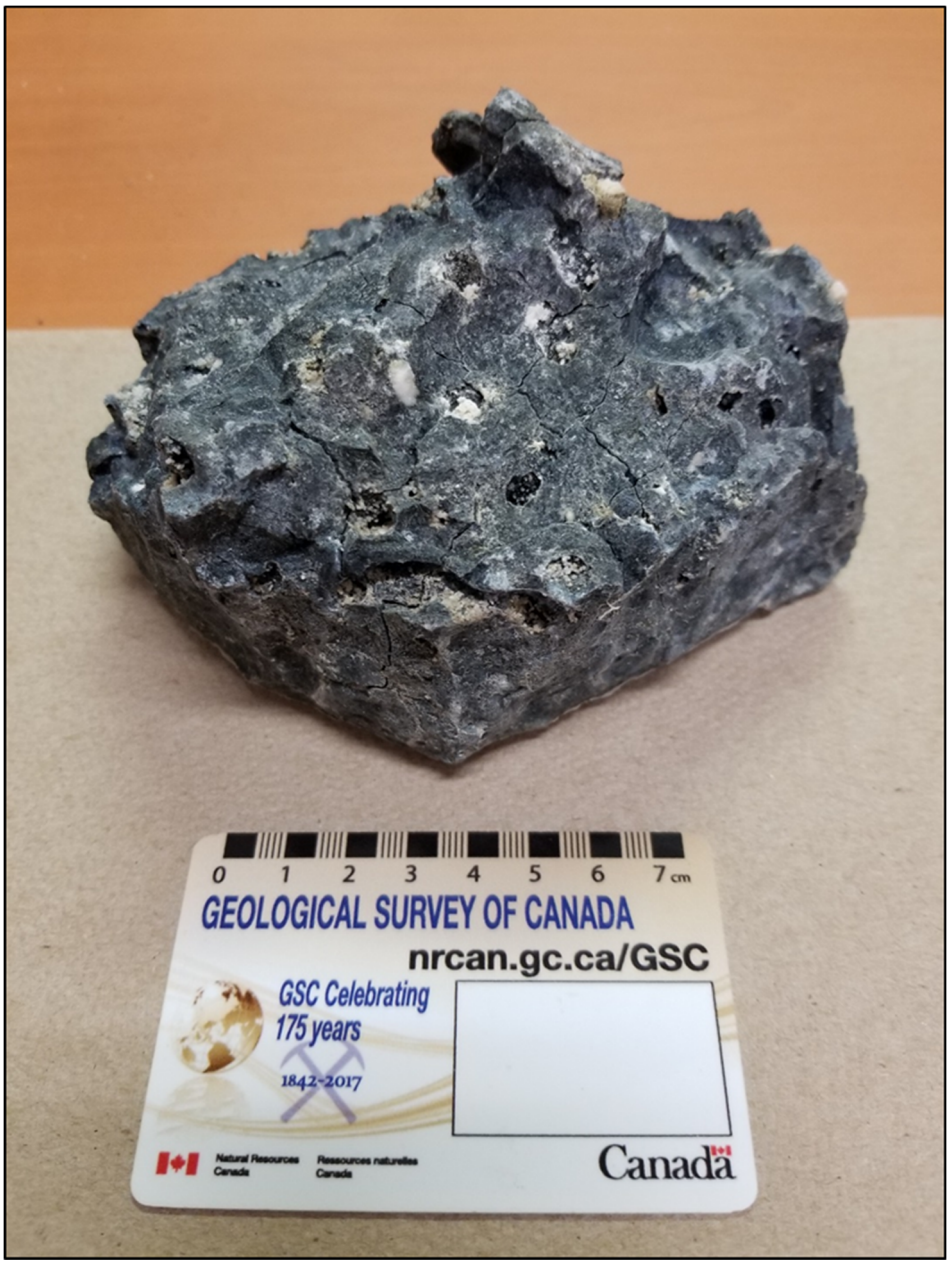

Figure A-9: Sample of highly weathered slag consisting of a dark grey, highly vesicular and pervasively cracked material. Some of the vesicles are partially or completely filled with a white mineral tentatively identified as gibbsite. Photograph by A.J. Desbarats. NRCan Photo Database number 2020-629.

Figure A-10: Sample of highly weathered slag. Opposite side of the sample in Figure A-9. The sample surface is a tan coloured rind with a ropy texture and a sand-paper roughness. Photograph by A.J. Desbarats. NRCan Photo Database number 2020-630.

Figure A-11: Sample of massive slag. This very fine-grained material is grey with greenish hues and shows little visible sign of weathering. Photograph by A.J. Desbarats. NRCan Photo Database number 2020-631.

Figure A-12: Sample of sponge-like slag. This material is a dark grey-green and shows little visible sign of weathering. Photograph by A.J. Desbarats. NRCan Photo Database number 2020-632.

Figure A-13: Sample of glassy slag. This material is a glossy black and shows little visible sign of weathering. Photograph by A.J. Desbarats. NRCan Photo Database number 2020-633.